SURFACE GRAFTING OF SYNTHETIC HYDROPHILIC POLYMERS VIA RING OPENING METATHESIS POLYMERIZATION FOR BIOMEDICAL APPLICATIONS

Stephanie Simone Stoddart

A thesis presented to the faculty of Mount Holyoke College
in partial fulfillment of the requirements for the degree of
Bachelor of Arts with honors

Department of Chemistry
South Hadley, Massachusetts
May 2005

This thesis was prepared under
the direction of Dr. Wei Chen
for 12 credits of independent study

We would like to thank National Institutes of Health for financial support

For Mom, Dad, Stephen and Andrew

ACKNOWLEDGEMENTS

I would like to thank my research advisor Professor Wei Chen for her support, encouragement and guidance. Working with Wei over the past two years has been an amazing experience. I am grateful for the support of my committee members: Professor Sean Decatur and Professor Craig Woodard. Sean, thanks for inspiring and motivating me. I will never forget the trouble I gave you in Quantum and Experimental Methods. Craig, Genetics was awesome. Because of you I have a greater appreciation for Biology. Mr. Thornsteinn Adalsteinson, "Mr T" your super critical comments have encouraged me to become a better scientist.

Anna, Rose and Kanchana, you girls are terrific lab partners. Kanch, thank you so much for your help with the norbornene studies. To my family and friends at home thanks for your love and support. Yo-Leigh, Christine and Anique thanks for always being there for me. Threshia, you are a great inspiration to me and I am really honored to have you as a friend. To Paejonette and Kimberly, thanks for keeping me alive with your madness at all hours of the night. Finally, to the person who knows me too well, words cannot express how much you mean to me.

TABLE OF CONTENTS

LIST OF FIGURES AND TABLES

Page Number

ABSTRACT

With increasing human life expectancy, the need for organ and tissue replacements has never been greater. People are living longer than before and human body parts are not keeping up since they are subject to injuries and diseases. Until tissue engineering becomes a reality, surgeons and researchers continue to rely on foreign replacement materials to address these problems. A key issue that researchers in the biomaterials field face is biocompatibility, in particular, blood compatibility of artificial implants in human bodies.

When a foreign object is implanted in the body, protein adsorption on the surface of the material takes place, which is followed by cell adhesion and numerous adverse biological responses such as coagulation, thrombosis, capsulation and inflammation. Researchers have focused mainly on designing protein-resistant materials as a key approach towards improving biocompatibility of artificial implants.

After almost two decades of research, it is now well known that poly(ethylene glycol) (PEG)-containing surfaces are resistant to protein adsorption, and are thus biocompatible. In this research, the synthetic neutral hydrophilic head-to-head poly(vinyl alcohol) (hh-PVOH) is grafted to silicon wafer surfaces and evaluated as a PEG alternative for biocompatibility. Norbornenyl groups are attached to surfaces via silanization followed by covalent attachment of Grubbs catalyst. hh-PVOH is synthesized by hydroxylation of polymers prepared from ROMP of cyclooctadiene. Polymer

chain length and chain density are controlled by silanization time, monomer concentration, and ROMP reaction time. Biocompatibility of these hydrophilic molecules can be assessed by protein adsorption. All of the surfaces are characterized by contact angle analysis, ellipsometry and x-ray photoelectron spectroscopy.

INTRODUCTION

The Demand for Biocompatible Materials

With increasing human life expectancy, the demand for organ and tissue replacements has never been greater. People are living longer than before and human body parts are not keeping up since they are subject to injuries and diseases. Until tissue engineering becomes a reality, surgeons and researchers continue to rely on artificial replacement materials to address these problems.[1] The solution is clear; but it is not as simple as it seems, since the human immune system presents a barrier to introducing foreign tissues. Consequently, a key issue that researchers in the biomaterials field face is biocompatibility, in particular blood compatibility, of artificial implants in human bodies. Materials with non-fouling, non-thrombogenic, biodegradable, bioinert properties are considered biocompatible. However, we do not understand enough as yet to obtain a precise definition of biocompatibility.

Over the last thirty years, significant effort has gone into research on biocompatible materials, and until now, the issue of blood compatibility remains a mystery.[2] When a foreign object is implanted in the body, protein adsorption on the surface of the material takes place, which is followed by cell adhesion and numerous adverse biological responses such as coagulation, thrombosis, capsulation and inflammation.[1,3] Researchers focus mainly on designing materials that prevent coagulation and thrombosis, the earliest and

most troublesome complications of these undesirable biological responses.[2] These cell-surface interactions are dependent on the properties of the implant material, surface coverage, composition, conformational state and biological status of the adsorbed proteins.[2] Therefore, control of protein interactions and in particular, control of nonspecific protein adsorption is one way of improving biocompatibility of artificial implants.[2]

The Current Approaches to Biocompatibility

The two most popular approaches of improving biocompatibility are: surface grating of poly(ethylene glycol) (PEG)[4] and designing phosphorylcholine-containing surfaces by grafting poly(2-methacryloxyethylphosphorylcholine) (PMPC) to mimic biomembranes.[5]

Poly(ethylene) glycol (PEG), a well-recognized biocompatible agent, is a synthetic, water soluble, nontoxic linear polymer with the chemical formula HO—$(CH_2CH_2O)_n$—H.[6] In aqueous environment, PEG is highly mobile and excludes other polymers from its presence. This results in protein rejection.[6] Covalently bound PEG molecules such as PEG-modified proteins and PEG-modified surfaces are also resistant to protein adsorption due to the inability of free proteins to approach these materials.[6] Nagaoka and coworkers were one of the first to study the adsorption of biological moieties to PEG surfaces. They found low protein adsorption and platelet adhesion to PEG hydrogels. After twenty years of research, it is now known that PEG-

containing surfaces are resistant to protein adsorption.[7] The exact mechanism of how PEG actually excludes proteins is still not well understood.

The design of biomembrane-like surfaces is another approach to improving biocompatibility of artificial implants. The rationale for engineering such surfaces lies in the fact that the phosphocholine head group of a phospholipid is the building block of the biomembrane surface.[4] In the fluid-mosaic model by Singer and Nicholson, amphiphilic phospholipids are asymmetrically arranged with a bilayer structure and proteins are located in or upon it.[4] Several attempts have been made to create a biomembrane-like surface that suppresses any biological response in blood. One of the relevant works is by Nakabayashi and coworkers in which they designed a methacrylate monomer with a zwitterion-type phospholipid polar group, 2-methacryloxyethylphosphorylcholine (MPC). MPC containing polymers are prone to phospholipids adsorption but are resistant to protein adsorption and cell adhesion.[8-10]

It has been shown that PEG-containing and MPC-containing surfaces are resistant to protein adsorption and cell adhesion.[7-10] Neutral PEG and amphipathic MPC interact differently with biological entities upon contact with body fluid. The Andrade-De Gennes theory proposed in 1991 accounts for the ability of PEG to resist protein adsorption. PEG surfaces are protein resistant because the contact between the protein and the surface causes the extended PEG chains to compress, thus decreasing its interaction with

surrounding water molecules. The decrease in entropy as a result of chain compression and an increase in enthalpy due to the decrease of hydration both serve to resist protein adsorption.

The mechanism that renders MPC-containing surfaces biocompatible differs from that of PEG-containing surfaces. MPC-type polymers are structurally very similar to natural phospholipids, and in the body they attract phospholipids. This association with natural phospholipids makes these MPC polymers appear similar to cell membranes and therefore do not trigger the body's defense system.[1] Although PEG and MPC are structurally very different they both make surfaces resistant to protein adsorption and cell adhesion. This observation begs the question, how does the molecular structure of these materials govern their non-fouling properties?

The Physical and Chemical Views of Biocompatibility

Non-fouling surfaces are surfaces that resist protein adsorption and cell adhesion. The mechanism of fouling resistance can be explained in terms of physical and chemical principles.[11] The physical view is based on the Alexander-De Gennes theory of polymer interfaces[12-14] and the chemical view is based on the limitations of the physical view.[11] It should be noted that these principles also explain the non-fouling characteristics of other surfaces besides PEG-containing ones.

The Alexander-De Gennes hypothesis is based on the theory of polymer interfaces and attributes fouling characteristics of PEG solely to entropic effects.[12-20] In this theoretical model, fouling resistant surfaces are viewed as having tethered and freely fluctuating chains of PEG that are resistant to adsorption and adhesion due to its large conformational freedom, i.e. the entropic effect. This paradigm only takes into account the free energies of steric repulsion, van der Waals attraction, and hydrophobic interactions and assumes that the effects of water are negligible.[15,16] The effects of water are negligible since water is assumed to be a good solvent for PEG. In addition, PEG has a low refractive index resulting in low van der Waals attraction with the protein.[15,16] Both van der Waals attractive forces and compressive forces exist at the protein-PEG interface.[15,16] According to this model, steric repulsion resulting from the compression of the PEG layer is the main mechanism driving protein resistance.[15,16] The limitations of this method lie in the fact that water is not taken into account as individual molecules. Hence it cannot account for some experimental results.

This theoretical model by Alexander-De Gennes[13,14] has since been revised by Szleifer.[17-20] The Szleifer approach based on a generalization of the single chain mean field theory takes into account the study of intramolecular and surface interactions in the PEG system. The protein approaching the surface is modeled as spherical in solution and the protein-polymer, protein-solvent, polymer-solvent interactions are all assumed to be

equal. Consequently, the interactions determining the structure of the layer and the protein-resistant properties of the coated surface are entirely repulsive. Since it is believed that no repulsive force other than that caused by the compression of the PEG-layer exists, any other force that gives rise to this compression is automatically assumed to be the one responsible for the protein-resistant properties.[17-20] Unlike the Alexander-De Gennes approach, the Szleifer method can reasonably predict most experimental results. This model accounted for the results obtained by Whitesides' group on oligoethyleneglycol (OEG) terminated self-assembled-monolayers (SAMs) in which PEG oligomers on gold substrates produced protein-resistant surfaces.[21]

The chemical view of fouling resistance is based on the shortcomings of the physical view, i.e. this model takes into account the effect of water. In the physical view models, the effect of hydrogen bonding, which is the key feature of water and water-soluble molecules, does not enter the picture. The effect of hydrogen bonding adds complexity to the earlier physical school of thought and sheds new light on the explanation of non-fouling surfaces. Hydrogen bonding between surfaces and water creates energy barriers that resist adsorption and thus gives rise to the non-fouling characteristics of surfaces.

The Besseling approach is the basis of the chemical view, which recognizes the orientation-dependent properties of the water molecule.[22-25] A water molecule is made up of an oxygen atom (electron donor) attached to

two hydrogen atoms (electron acceptors). The presence of these electron-donor/electron-acceptor sites determines water's orientation-dependent properties and thus dictates the interactions at the solid-solution interface. The presence of lone pairs of electrons on the oxygen atoms of the repeating unit of PEG accounts for PEG's basic characteristics. When water molecules approach a PEG-containing surface they hydrogen bond with PEG giving rise to attractive hydration forces. On the other hand, repulsive hydration forces are associated with the disruption of hydrogen bonding which occurs when proteins adsorb onto water-soluble molecules on the surface to replace hydrogen bonded water molecules.[22-25]

The physical and chemical schools of thought can both be used to explain the non-fouling properties of biomaterials. The main difference between the two is the origin of the force felt by a protein. The physical view focuses on entropic effects whereas the chemical view focuses on the perturbation of the hydration layer by water-soluble molecules such as PEG and MPC on surfaces.[11]

Water is a universal solvent and as such its presence plays an important role in its interaction with water-soluble molecules on surfaces. As pointed out by the chemical view, protein resistance of biomaterials is directly related to the resistance of surface groups to release their bound water molecules. Hence it seems only logical that most approaches to reduce

protein adsorption and cell adhesion of biomaterials are to make them more hydrophilic.[26]

Our Approach to Other Biocompatible Molecules

In this study, head-to-head poly(vinyl alcohol) (hh-PVOH), a synthetic hydrophilic polymer, which has never been prepared, was grafted to silicon wafer surfaces in order to further understand the fundamentals of the non-fouling phenomenon and to assess its biocompatibility as a substitute for PEG. The selection rationale for the substrate is based on the fact that hh-PVOH is a hydrophilic polymer containing –OH groups which can hydrogen bond with surrounding water molecules. Furthermore, silane chemistry is well-understood and surface characterization techniques such as contact angle, ellipsometry, atomic force microscopy (AFM) and x-ray photoelectron spectroscopy (XPS) can be used to quantify the amount of hh-PVOH on silicon. Most biological reactions take place on surfaces and the rules that govern biological surface phenomena are the same as those which govern reactions at a silicon surface and as such it is the substrate of choice.[3]

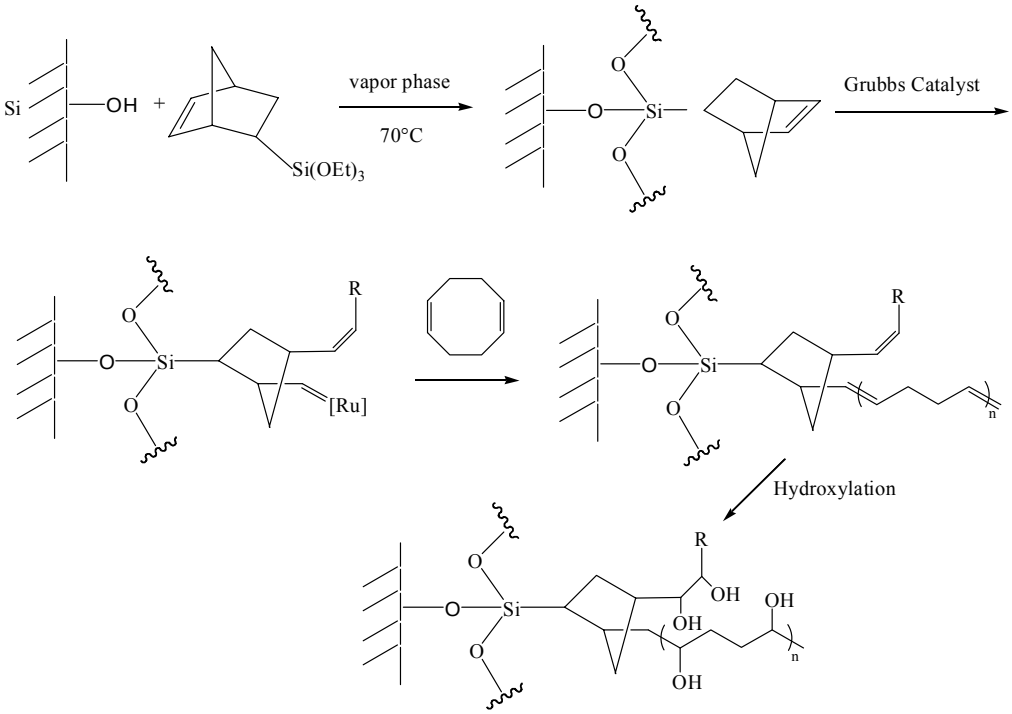

Figure 1. Synthetic routes of head-to-head poly(vinyl alcohol)

The reaction scheme for the synthesis of hh-PVOH is shown in Figure 1. Monolayers of norbornenyltriethoxysilane were prepared by the reaction of the silane with silicon wafers. Grubbs catalyst attachment, followed by ring opening metathesis polymerization (ROMP) using the monomer cyclooctadiene (COD) gave rise to polycyclooctadiene. hh-PVOH was obtained after hydroxylation of poly(COD). Protein adsorption studies can be performed on hh-PVOH in order to determine its ability to resist proteins and cells.

Silanization

Surface modification of inorganic materials using reactive organosilanes is widely used in both research and technology.[27] Modification of these surfaces enables researchers to control features such as wettability, colloid stabilization, fabrication of chemical microsensors, surface activity and biocompatibility.[28] Different structures can be produced on surfaces depending on reaction conditions, chemistry of the organosilanes and surface history.[29] Monomeric alkyl-bonded reversed-phase chromatography stationary phases and self-assembled monolayers are two areas of research which have highly evolved.[27] Monofunctionalized silanes (R_3SiX where X = Cl, OR, NMe_2) have been used to prepare chromatographic stationary phases on porous surfaces; while self-assembled monolayers on single surfaces have been prepared with tri-functionalized ones ($RSiX_3$).[27,28]

Monofunctionalized organosilanes offer greater control over the modification of surface properties as opposed to their tri-functionalized counterparts. The substrates prepared with monofunctionalized silanes are more reproducible since only one reactive site is available for surface attachment.[28] Trifunctionalized organosilanes are more reactive than monofunctionalized ones and thus give rise to a number of possible surface structures and hence are more difficult to control.

Silanization can be achieved both in vapor and solution phases. Parameters such as temperature, solvent and surface water are taken into

account depending on the chosen reaction condition. Surfaces prepared in both vapor and solution phases are the same in thickness. Reaction condition depends on the type of silane used as well as the goal of the project. In this project, the silane used is tri-functionalized and water sensitive so we employed the vapor phase condition to ensure a better control of the amount of adsorbed water.

Ring Opening Metathesis Polymerization

The applications of a polymer are determined by its morphology, which depends on its composition and architecture. Ring opening metathesis polymerization (ROMP) is chosen instead of other living polymerization methods because of its ability to offer greater control over the polymer microstructure, stereochemistry and molecular weight.[30] ROMP is a type of living polymerization in which metal-carbene complexes with the formula $L_nM=CHR$ (based on ruthenium and molybdenum) break the double bond of a cyclic olefin and convert the ring-opened molecule into a polymer with double bonds in the main chain.[31] ROMP generates living polymers primarily with trans double bond configuration (Figure 2).[32] During ROMP, the catalyst forms a Ru^{2+}-monomer complex (M) which is regenerated at each cycle.

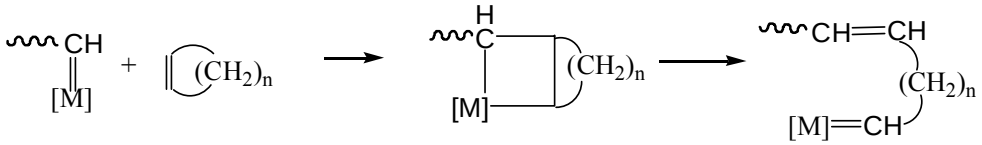

Figure 2. Propagation step of ROMP[32]

Schrock et al.[31] developed the first set of catalysts for ROMP, which was based on the highly active group VI metals. Although these catalysts provided control over the polymer microstructure, they were difficult to characterize. More recently, Grubbs and coworkers developed ruthenium-based catalysts that allow the metathesis reactions in polar and nonpolar reaction media.[30] These catalysts are most commonly used because of their tolerance towards oxygen, water and impurities.[31] It is now known that the rate of polymerization is a function of metal carbene reactivity.[32] Consequently, in our study, polynorbornenes obtained via ROMP using Grubbs catalyst generations I and II were compared in an effort to optimize the reaction conditions for the cyclooctadiene system. Another reason for the choice of norbornene and 1,5-cyclooctadiene monomers in this study is because they possess ring strains of 27.2 kcal/mol and 13.28 kcal/mol respectively, and therefore undergo ROMP.[33] Surface-initiated ROMP (SI-ROMP) has been carried out on Au, Si and Si/SiO_2 surfaces using Grubbs catalyst generation I.[34]

Surface Characterization Techniques

The chemistry of a material determines its structure, which in turn determines properties such as biocompatibility. Techniques such as ellipsometry, contact angle analysis, and x-ray photoelectron spectroscopy (XPS) were utilized in this study to determine chemical structure and hydrophilicity/hydrophobicity of the prepared surfaces.

The thickness of a substrate layer gives us information on how much product has been grafted to the surface and as such ellipsometry was employed. This technique is based on the principles of polarized light. Light is said to be polarized if its electric field lies in the same plane. Two light beams polarized in the same plane with the same frequency along the same path in phase combine to give a resultant linearly polarized wave. If their electric fields are perpendicular to each other and the phase difference is 90° (A and B), the resultant wave C (Figure 3) would appear to be a circle if you looked end on. A phase difference other than 90° gives elliptically polarized light.[35]

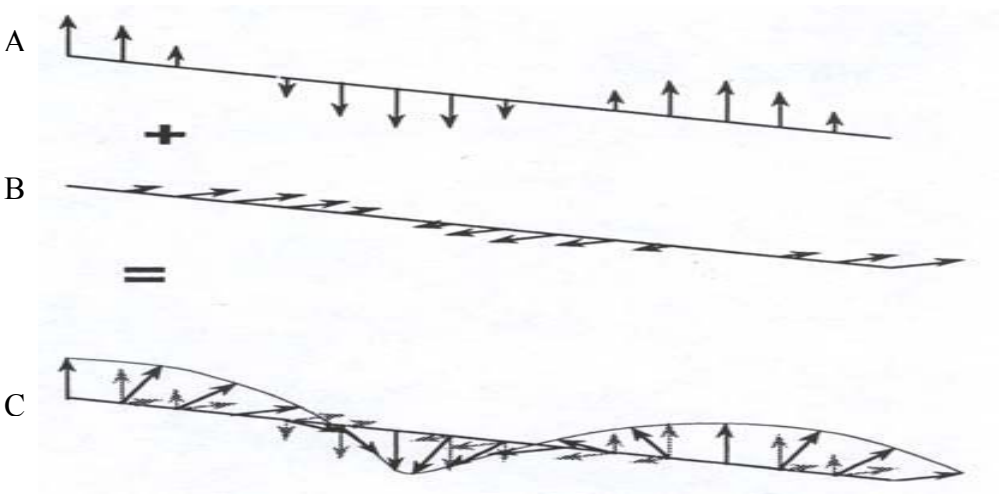

Figure 3. Two linearly polarized light beams out of phase combine to give a resultant wave that is elliptically polarized.

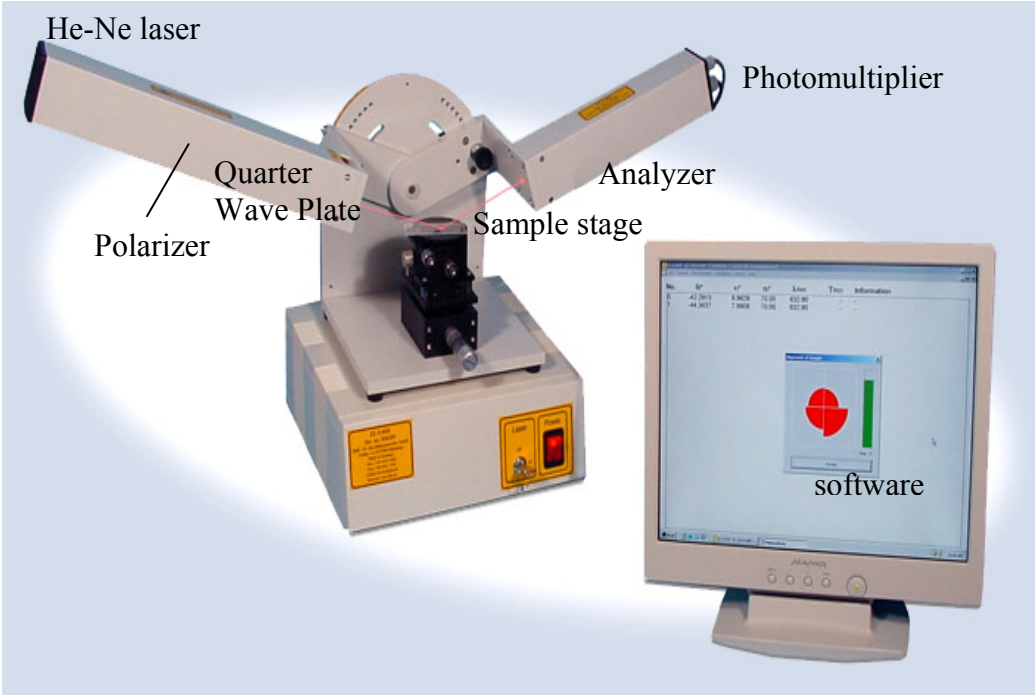

Figure 4. Ellipsometer

A monochromatic light source (in the form of He-Ne laser), polarizer, quarter wave plate, sample stage (which provides reflection from the sample of interest), analyzer, photomultiplier and calculation software (Figure 4) are all requirements for ellipsometry.

The laser light source is unpolarized and travels through a polarizer that polarizes it. The quarter wave plate fixed at an angle of 45° converts linearly polarized to elliptically polarized light. Elliptically polarized light hits the SiO_2 layer (silicon wafer sample) some is reflected at an angle of Φ_1 and the rest is refracted at an angle of Φ_2. This refracted light hits the Si layer and can be reflected and refracted. The latter gets refracted again and returns to the analyzer with a combination of changes in phase differences and amplitudes (Figure 5).

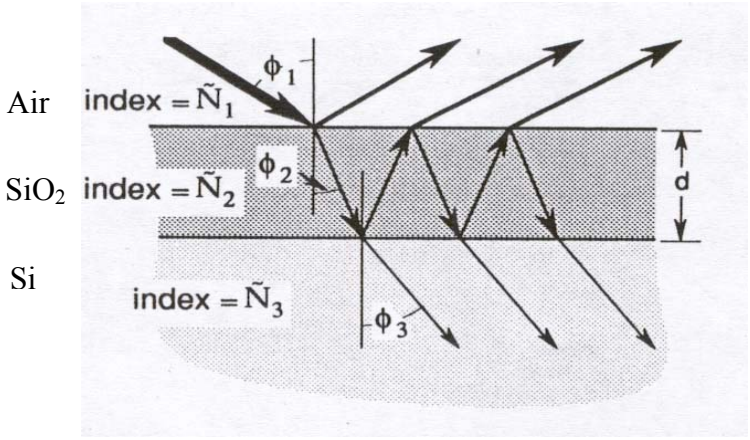

Figure 5. Reflection and refraction at multiple interfaces

The analyzer and polarizer are both rotated until the null is found which allow us to calculate Delta and Psi. Delta (Δ) is the change in phase

difference that occurs upon reflection and its value can be from 0° to 360°. Psi (Ψ) is the angle whose tangent is the ratio of the magnitudes of the total reflection coefficients. The value of Ψ can be between 0° and 90°. The fundamental equation of ellipsometry is $\tan\psi e^{j\Delta} = \frac{R^p}{R^s}$ where R^p is the amplitude of the outgoing wave for the parallel component and R^s is the amplitude of the outgoing wave for the perpendicular component. Ψ and Δ are quantities measured by the ellipsometer.[35] Thickness or refractive index of surface layers can be calculated based on these parameters.

Protein adsorption can be influenced by wettability. Contact angle analysis, a common and useful measure of wettability, was employed in this study to assess the hydrophilicity of the system. This technique gives information about the energetics, roughness and heterogeneity of the outermost few angstroms of the surface.

Thomas Young in 1805 related contact angle to the surface energies of the solid and the liquid, and Gibbs later explained the thermodynamics of this system in 1878.[36] Surface phenomena are associated with a reduction in surface free energy and a liquid drop on a solid substrate takes the shape that minimizes the free energy of the system.[36] For a plane, smooth, nondeformable surface the minimization gives rise to Young's equation. The surface free energy of the solid-liquid interface (γ_{SL}), the surface free energy of the solid-vapor interface (γ_{SV}) and the surface free energy of the liquid-

vapor interface (γ_{LV}) need to be in equilibrium in order to determine the intrinsic contact angle (θ) independent of how the angle is measured (Figure 6).[36]

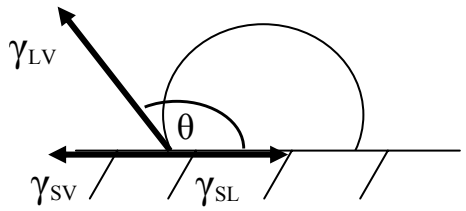

$$\cos\theta = \frac{\gamma_{SV} - \gamma_{SL}}{\gamma_{LV}}$$

Figure 6. Surface free energies of the solid-vapor, solid-liquid and liquid-vapor interfaces at equilibrium

The situation described above represents an idealized one in which there is only one equilibrium contact angle. In real systems, it has been observed that a number of stable angles can be measured, the two most reproducibly ones being advancing and receding angles.[37] Dynamic advancing (θ_A) and receding (θ_R) contact angles are measured while the probe fluid is added to and withdrawn from the drop, respectively (Figure 7). Hysteresis, the difference between these two angles (θ_A-θ_R), provides information about the heterogeneity and roughness of the surface.[36,37]

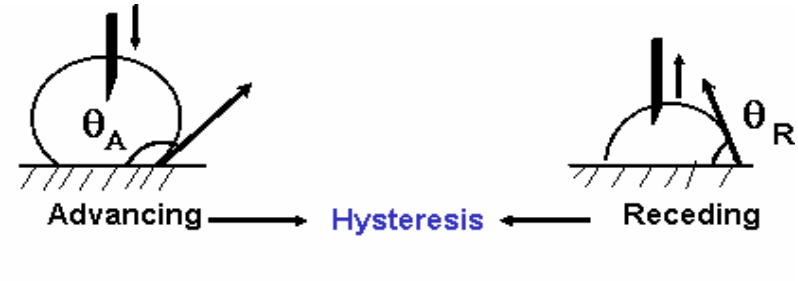

Figure 7. Measurement of advancing (left) and receding (right) contact angles

Contact angle hysteresis can be categorized according to thermodynamic and kinetic influences. Thermodynamic hysteresis describes contact angle measurements that are reproducible with the same liquid on the same substrate. This type of hysteresis can be used to predict surface roughness and heterogeneity. Kinetic hysteresis, being time dependent, is observed when hysteresis changes as θ_A approaches θ_R with repeated contact angle measurements.[36,37]

Contact angle measurements can be carried out using a variety of techniques such as sessile drop, captive bubble, and Wilhelmy plate methods. The sessile drop method is commonly used in analyzing the hydrophilicity/hydrophobicity of biomaterials. In this method, the contact angle measurement is made by determining the angle between the surface and the tangent of a liquid drop at the point of contact with the solid substrate (Figure 6).[37]

X-ray photoelectron spectroscopy (XPS) is used to determine the chemical composition of solid surfaces. In addition to providing elemental

information, XPS also gives information concerning the relative amounts of functional groups present on a surface.[36] The principle of XPS is based on the photoelectric effect, in which a beam of monochromatic x-rays is used to irradiate a surface resulting in the emission of core shell electrons (Figure 8).[36,38] XPS is a very sensitive surface technique since only electrons from the outer few nanometers of the surface are able to escape without losing their kinetic energy from inelastic collisions with the bulk.[36] These emitted electrons are then quantified as a function of their kinetic energy. Since there is a characteristic binding energy for each core electron an elemental analysis is obtained.[36,38]

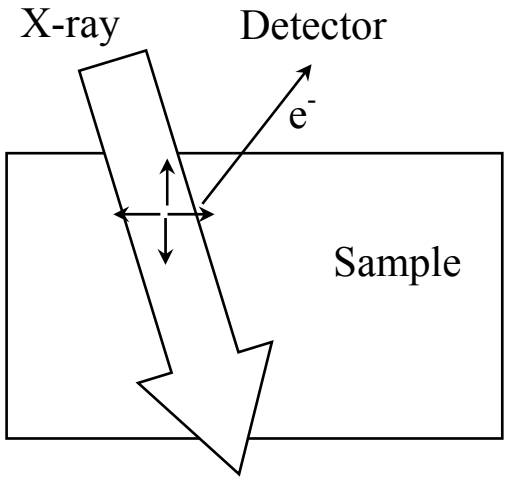

Figure 8. Irradiation of a sample of interest with x-ray

The binding energy of core electrons, E_{BE}, which is characteristic of the element and bonding environment, can be calculated using the following equation:

Binding energy = incident x-ray energy – photoelectron kinetic energy-work function or

$$E_{BE} = h\nu - E_{KE} - \varphi$$

where h is Planck's constant, ν is the light frequency of irradiation, φ is the work function, E_{KE} is the specific photoelectron kinetic energy and E_{BE} is the binding energy. The binding energies for core electrons range from 0-1000 eV. As a result, the incident ray should produce light with energy greater than 1000 eV or the soft x-ray range.

XPS is a particularly versatile technique for analyzing samples at different depths. This method involves varying the take-off angle θ between the sample and the detector (Figure 9). Measuring the photoelectron intensities at different take-off angles provides further information regarding the compositional variation as a function of depth. Variable angle XPS proves to be very useful for samples that have a surface excess of one material over another.[36] It can also be used to examine a layer that is not uniform, or to study the change between bulk and surface of a 'surface modified' material.[38] As shown in Figure 9, the sample is probed more deeply (~40 Å) at the larger take-off angle of 75° assuming the same distance that electrons can travel before reaching the solid/air interface. Conversely, at the smaller take-off angle of 15°, fewer electrons can escape from the deeper regions without losing their kinetic energy due to inelastic collisions with the sample matrix before reaching the detector; the sampling depth is only ~10 Å.[36]

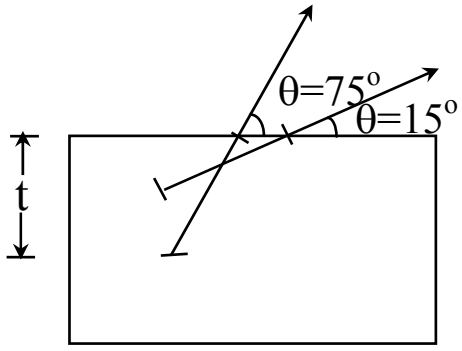

Figure 9. Variable angle XPS

The number of electrons detected from any depth may be expressed as:

$$\frac{N}{N_o} = e^{-\frac{t}{\lambda \sin\theta}}$$

where N_o is the number of electrons originating at depth, t , N is the number of electrons emitted from the solid, λ is the mean free path of the electron and θ is the take-off angle.

EXPERIMENTAL

General. Silicon wafers were obtained from International Wafer Service (100 orientation, P/B doped, resistivity 1-10 Ωcm, thickness 450- 575 μm). 5-(bicycloheptenyl)triethoxysilane was purchased from Gelest, transferred to custom-built Schlenk tubes and stored under nitrogen. Heptafluorbutyrylchloride (HFBC) (95%) was purchased from Aldrich, transferred to a custom-built Schlenk tube and stored under nitrogen. Toluene (HPLC grade), ethanol (HPLC grade), hydrogen peroxide (30%), sulfuric acid (concentrated), and sodium dichromate were used as received from Fisher. Toluene (anhydrous), benzylidene-bis(tricyclohexylphosphine)dichlororuthenium (Grubbs catalyst- 1st generation), 1,3-bis-(2,4,6-trimethylphenyl)-2-imidazolidinylene)dichloro(phenylmethylene)-tricyclohexylphosphine)ruthenium (Grubbs catalyst- 2nd generation), norbornene, ethyl vinyl ether, osmium tetroxide, 2-methyl-2-propanol (t-BuOH), tetraethylammonium acetate tetrahydrate (TEAA), t-butyl hydroperoxide (t-BuOOH), *meta*-chloroperoxybenzoic acid (MCPBA) (77%) were purchased from Aldrich and used as received. Perchloric acid (70%) was purchased from Acros Organics and used as received. Redistilled 1,5-cyclooctadiene (COD) was purchased from Aldrich and was degassed by bubbling nitrogen through for 30 min before use. House purified water

(reversed osmosis) was further purified using a Millipore Milli-Q system that involves reversed osmosis, ion exchange and filtration steps (10^{18} Ω/cm).

Instrumentation. X-ray photoelectron spectra (XPS) were recorded with a Physical Electronics Quantum 2000 ESCA Microprobe with Al K_α excitation. Spectra were obtained at 15°, 45°or 75° take-off angles (between the plane of the surface and the entrance lens of the detector optics). Contact angle measurements were made with a Ramé-Hart telescopic goniometer and a Gilmont syringe with a 24-gauge flat-tipped needle. The probe fluid used was water, purified as described above. Dynamic advancing (θ_A) and receding angles (θ_R) were recorded while the probe fluid was added to and withdrawn from the drop, respectively. Ellipsometric measurements were made with a Microphotonics EL X-01R ellipsometer. The light source is a He-Ne laser with $\lambda = 632.8$ nm. The angle of incidence (from the normal to the plane) is 70°. The thickness of the layers is calculated using a single layer model (silicon substrate/silicon oxide + graft layers/air) with the following parameters: air, $n_0 = 1$; silicon oxide + graft layers, $n_1 = 1.457$; silicon substrate, $n_s = 3.882$, $k_s = 0.019$ (imaginary part of the refractive index).

Pretreatment of Silicon Substrates/Surface Cleaning. Silicon wafers were cut into 1.5 cm x 1.3 cm pieces. The samples were first dusted using compressed air, rinsed with reversed osmosis water and dried with compressed air. These samples were then placed in a custom-designed slotted-hollow-glass cylindrical holder and submerged in a freshly prepared 1

part of concentrated sulfuric acid containing ~2 wt% sodium dichromate and 1 part of 30% hydrogen peroxide for 1 h. Upon preparation, the solution turns green, gives off heat and effervesces due to the formation of oxygen and ozone. Wafers were then removed and rinsed with copious amounts of water and dried in a clean oven at 110 °C for 30 min. Thickness of the native oxide on clean wafers was determined to be ~ 22 Å by ellipsometry.

Reaction of Silicon Wafers with Norbornenyltriethoxysilane in Vapor Phase. The reagent flask containing norbornenyltriethoxysilane was purged under nitrogen for 1-2 min using a cannula (Figure 10). The outer end of the cannula was then placed at the bottom of a clean Schlenk tube and the reagent stopcock was opened. The cannula was inserted in the liquid silane and ~ 0.5 mL of silane was transferred. Clean silicon wafers were placed in a custom-built glass holder and introduced to the Schlenk tube with no contact between the samples and the silane. The Schlenk tube was closed and subsequently placed in an oil bath at 70 °C for the desired amount of time. After silanization, wafers were rinsed with toluene (3x). One sample out of each batch was reserved for characterization by ellipsometry, contact angle and XPS.

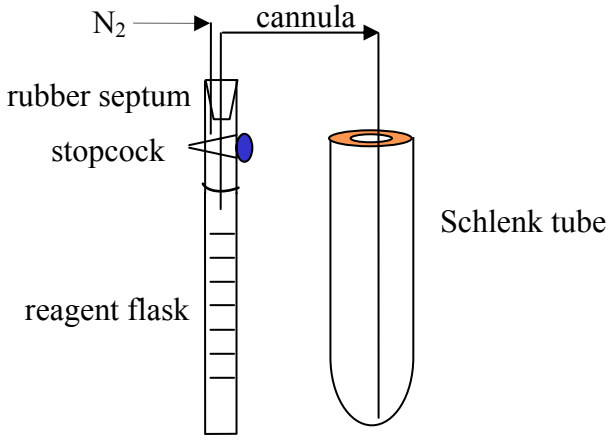

Figure 10. Schematic diagram depicting the transfer of a liquid silane

Catalyst Attachment and Ring Opening Metathesis Polymerization of Norbornene.

Grubbs catalysts (generations I and II) were stored in a desiccator in a nitrogen filled glove bag. Before use, the glove bag was purged three times with nitrogen before the desired amount of catalyst was transferred to a Schlenk tube. The Schlenk tube was subsequently closed and taken to a hood for use. Anhydrous toluene was transferred to the tube via a cannula to produce ~ 1 mM Grubbs catalyst toluene solution. The Grubbs catalyst generation I solution is light purple and the Grubbs catalyst generation II solution is reddish brown. The colors of the solutions darkened upon exposure to air. The silane-containing substrates were immersed in this solution for 30 min at room temperature under nitrogen. They were then rinsed once in HPLC grade toluene. The desired amounts of norbornene and anhydrous toluene were transferred to a Schlenk tube. The catalyst-attached

wafers were immediately immersed in the norbornene/anhydrous toluene solution for the desired amount of time at room temperature under nitrogen. ~ 0.5 mL of ethyl vinyl ether was injected to terminate polymerization. Wafers were then rinsed with toluene (2x), ethanol and water. They were subsequently dried at reduced pressure for 30 min.

Catalyst Attachment and Ring Opening Metathesis Polymerization of Cyclooctadiene.

The silane-containing substrates in a custom-built glass holder and a Schlenk tube were placed in the glove bag. Before use, the glove bag was purged three times with nitrogen before the desired amount of Grubbs catalyst generation II and the samples were transferred to the tube. The tube was subsequently closed and taken to the hood for use. Anhydrous toluene was transferred to the tube via a cannula and the tube was shaken vigorously to produce ~1 mM Grubbs catalyst toluene solution. After 30 min at room temperature, this Grubbs catalyst toluene solution was transferred out of the tube via a cannula. Fresh anhydrous toluene was transferred to the tube via a cannula and the tube was shaken vigorously to remove excess catalyst before the solution was transferred out. Redistilled COD was first degassed by bubbling nitrogen through the liquid for 30 min and then transferred to the sample tube. Polymerization of COD was run neat for the desired amount of time at room temperature under nitrogen.

***Cis*-dihydroxylation - Osmium Tetraoxide.** Osmium tetroxide (OsO_4) solution was prepared by dissolving 250 mg of OsO_4 and 0.25 mL of t-butyl hydroperoxide (t-BuOOH) in 50 mL of 2-methyl-2-propanol (t-BuOH). A reaction mixture containing 0.25 g of tertaethylammonium acetate tetrahydrate (TEAA) in 30 mL of water-acetone mixture (3:1), 0.1 mL H_2O_2 and 0.2 mL OsO_4 solution kept at 0°C was introduced to a Schlenk flask containing samples with grafted polymers. After 30 min at 0°C, the samples were warmed up to room temperature and the reaction was carried out for a total of 2 h. The hydroxylated samples were rinsed with a copious amount of water, vacuum-dried for 30 min, and then characterized using ellipsometry, contact angle analysis and XPS.

***Trans*-dihydroxylation – *meta*-Chloroperoxybenzoic Acid (MCPBA).** 1 g of MCPBA was dissolved completely in 20 mL toluene. Samples with grafted polymers were introduced to this solution and left to react overnight under stirring. After epoxidation, the samples were rinsed with excess amounts of toluene. One sample out of the batch was taken out for characterization by ellipsometry, contact angle analysis and XPS. The remaining samples were introduced to a solution containing 0.7 mL of perchloric acid in 26 mL of water and reacted for 7 h. After hydrolysis, the samples were rinsed with a copious amount of water, vacuum-dried for 30 min and characterized by ellipsometry, contact angle analysis and XPS.

Labeling with Heptafluorobutyryl Chloride (HFBC).

Hydroxylated samples were reacted with HFBC overnight in the vapor phase at room temperature. These samples were rinsed with excess amounts of water, vacuum-dried and characterized by ellipsometry, contact angle analysis and XPS.

RESULTS AND DISCUSSION

Living polymerizations, processes in which there are neither chain transfers nor terminations, offer the distinct advantage of low polydispersity, uniform surface grafting density and linear polymer chains as opposed to their nonliving analogues.[39] Until the recent discovery of well-defined metal-alkylidines, which catalyze ring-opening metathesis polymerization (ROMP), surface living polymerizations had not been successful due to side reactions and surface impurities.[39,40] These ruthenium-based ROMP initiators give researchers precise control of polymer length and low polydispersity.[39] Kim et al. synthesized polynorbornene films from the native silicon oxide of silicon wafer surfaces via ROMP.[41] Surface-initiated ROMP of norbornene has been discussed in other recent literature.[39, 42]

In our study, silicon wafer surfaces were first oxidized using a hydrogen peroxide/sodium dichromate/ sulfuric acid solution (see the Experimental section). Norbornenyl groups were introduced to clean silicon wafer surfaces by silanization with norbornenyltriethoxysilane in the vapor phase at 70 °C. Norbornenyltriethoxysilane results in more controllable silane layer thickness than the corresponding trichlorosilane. Alkyltrichlorosilanes are more reactive and can undergo horizontal polymerization (self-assembly), vertical polymerization and covalent attachment with surface silanols hence their silane layer thicknesses are uncontrollable.[29] Vapor phase reactions as opposed to solution phase reactions produce a sub-to complete monolayer of

the silane with controllable norbornenyl group density. Vapor phase reactions were used over solution phase ones since this method appeared to be the cleanest and easiest method to obtain high yield surface modification.[27] Vapor phase reactions are not as applicable for silanes with low vapor pressure[42] so using high reaction temperatures is necessary at times.

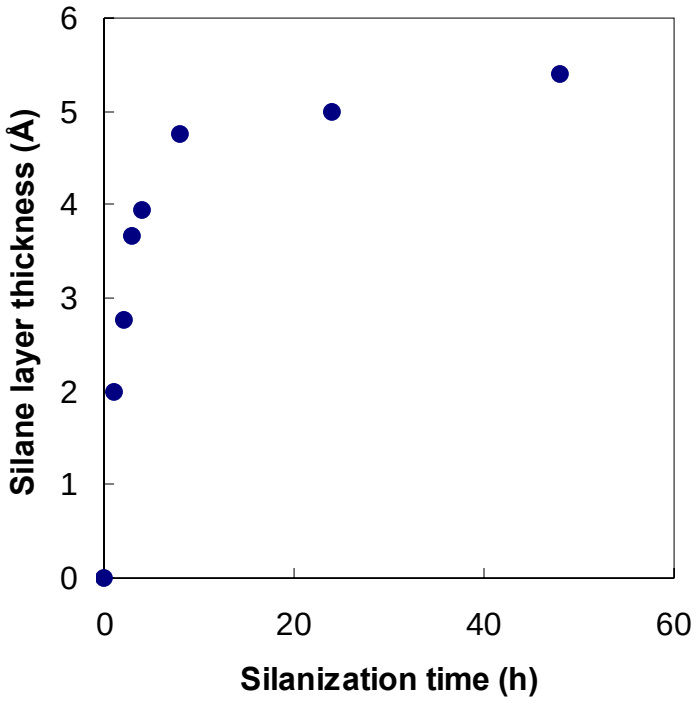

Figure 11. Kinetic study of silanization of norbornenyltriethoxysilane

Figure 11 shows the silane layer thickness as a function of silanization time. As silanization time increases there is a corresponding increase in the silane layer thickness. Silane layer thickness increases almost linearly up to silanization time of 4 h. The largest silane growth occurs between t = 0 h and

t = 1 h. This is expected since clean silicon wafers contain high-energy silanol groups, which are quickly reacted with norbornenyltriethoxysilane. Silane thickness increase slows down after 4 h. After a silanization time of 8 h, the thickness increase slows down even more; a silane layer thickness of 5-6 Å which corresponds to a monolayer of norbornenyl groups is obtained after 48 h. This trend can be explained more succinctly if the throwing darts analogy is used. It is very easy to throw a dart at an empty dartboard, which is analogous to silane groups being deposited on the surface initially. If the dartboard is almost covered with darts it is harder for a dart to land at an empty spot. In our case, after silanization time of 8 h it is harder for the silane group to be deposited at an empty/available spot. Based on this kinetic study, a silanization time of 24 h was chosen as it afforded us a reproducible silane layer.

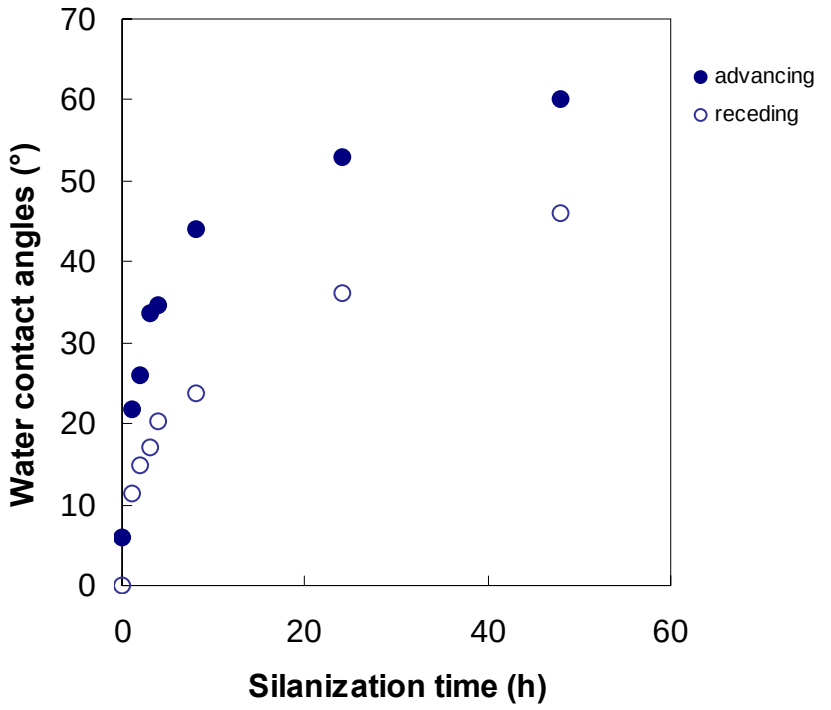

Figure 12. Advancing (●) and receding (○) water contact angles of grafted norbornenyltriethoxysilane samples prepared in vapor phase at 70 °C

Water contact angle analyses were conducted on the norbornenyl-containing samples to assess the hydrophilicity/hydrophobicity of the system. The observed trend of increasing water contact angles with increasing silanization time in Figure 12 corresponds well with Figure 11. An advancing angle of 53° and a receding angle of 36° are obtained for silanization time of 24 h. The contact angles suggest that this system is more hydrophobic than clean silicon wafers which is intuitive since the norbornenyl groups are more hydrophobic than the silanol groups (see Figure 1 for the silane structure).

The other parameter that was taken into consideration was the type of ROMP catalyst. Grubbs catalyst generations I and II (Figure 13) are two of the most widely used ROMP initiators.

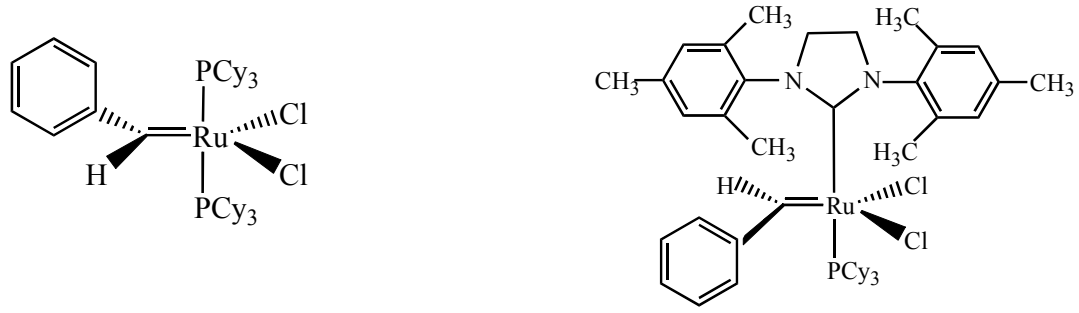

Figure 13. Grubbs catalyst generations I (left) and II (right)

Dias et al. [43] conducted a study to determine the mechanism of ruthenium-mediated olefin metathesis. It was later established in 2001 by Sandford et al[43] that phosphine dissociation occurred before olefin binding. In the mechanism of ruthenium-mediated olefin metathesis, initiation takes place by loss of phosphine (PR_3) from the complex (I) (Figure 14).

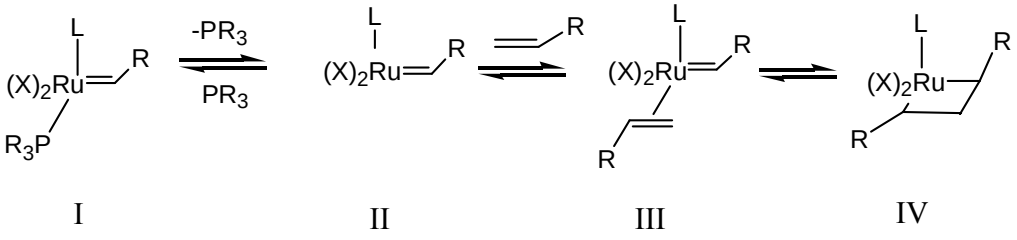

Figure 14. Mechanism of ruthenium-mediated olefin metathesis[43]

This intermediate (II) can proceed via two pathways: it can rebind phosphine or it can bind olefin. The complex (I) is recovered from the cycle if the intermediate rebinds phosphine (PR_3). Conversely, reaction of the intermediate (II) with olefin continues the catalytic cycle (Figure 14). It was reported that the rate of initiation of Grubbs catalyst generation I is approximately two orders greater than that of generation II. However, the rate of metathesis catalyzed by generation II is about two orders greater than that of generation I. Fast initiation and relatively slow propagation of generation I results in polymers with relatively uniform chain lengths. More specifically, polymers prepared from Grubbs catalyst generation I have polydispersities (PDIs) around 1.2 whereas polymers with uncontrolled molecular weights and broad PDIs are obtained using Grubbs catalyst generation II.[44] Based on these differences, polymers were prepared from both Grubbs catalyst generations I and II in order to determine the operating conditions for the polynorbornene and polycyclooctadiene systems.

Most of these reported studies were not conducted on surfaces; therefore in order to ensure the success of the catalyst attachment step XPS spectra were obtained (Figure 15).

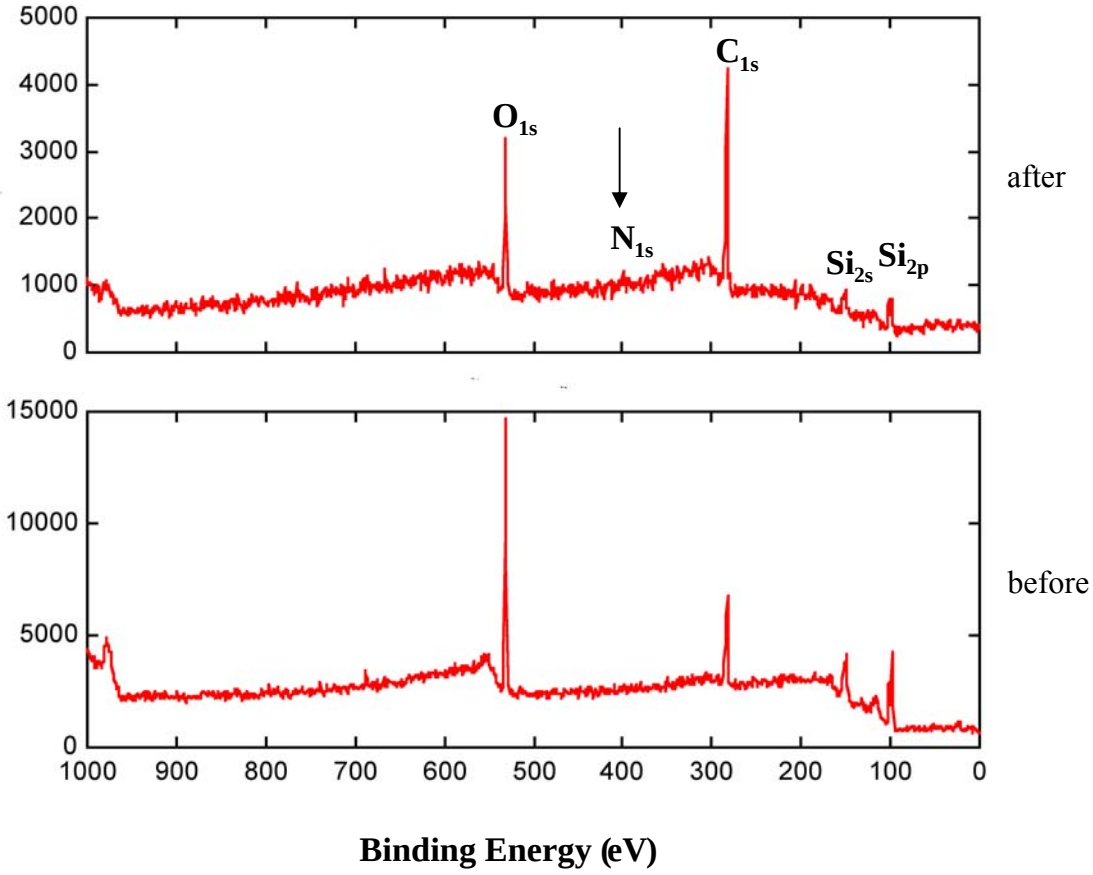

Figure 15. XPS spectra of 1 h silanized samples obtained at 15° take-off angle before (bottom) and after (top) the attachment of Grubbs catalyst generation II

The presence of a small N_{1s} peak (1.9 %) at ~ 400 eV is indicative of the attachment of Grubbs catalyst generation II which contains a N-heterocyclic carbene ligand (See Figure 13 for the catalyst structure). The decrease of the Si_{2p} and O_{1s} signals of the substrate after the reaction also indicates the presence of the catalyst (Table 1). The catalyst is rich in carbon content and the almost two-fold increase of the C_{1s} signal further confirms its presence. The Ru_{3d} peak could not be resolved from the C_{1s} peak.

Table 1. Ellipsometric thickness, XPS elemental composition at 15° take-off angle and water contact angles for 1 h silanized samples before and after attachment of Grubbs catalyst generation II

Substrate	Thickness increase (Å)	C_{1s} (%)	O_{1s} (%)	Si_{2p} (%)	N_{1s} (%)	θ_A (°)	θ_R (°)
SiO_2	22 ± 2	3.2	61.3	35.5	-	6	0
Norbornenyltriethoxy silane	2 ± 0.42	34.5	39.4	26.2	-	22	12
Grubbs catalyst	~3	63.6	22.0	12.5	1.9	77	45

Key: - does not contain element

Molecular weight of a polymer is controlled by the monomer concentration as well as polymerization time. Concentration and kinetics studies were conducted using both Grubbs catalyst generations I and II. Grafting reactions were carried out using 0.040 to 0.318 M norbornene/toluene solutions for Grubbs catalyst generation II-containing substrates overnight. As illustrated in Figure 16 polynorbornene films up to ~ 900 Å are obtained for Grubbs catalyst generation II. As norbornene concentration increases there is a corresponding linear increase in the thickness of polynorbornenes, which indicates that the polymerization initiated with Grubbs catalyst generation II is a living polymerization.

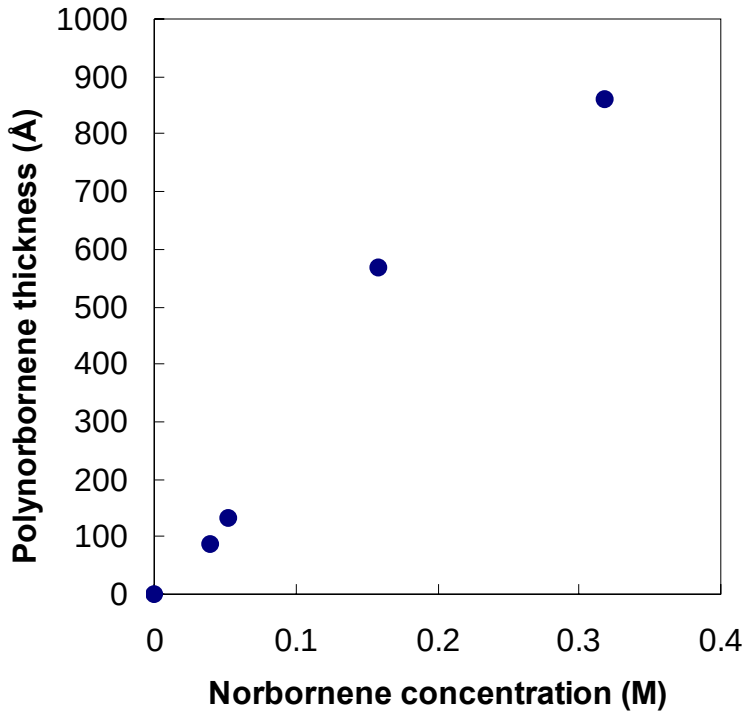

Figure 16. Ellipsometric thickness of polynorbornenes prepared using Grubbs catalyst generation II as a function of norbornene concentrations in toluene

The grafted polynorbornenes are hydrophobic and very closely packed together and as such water contact angles of ~ 85°/ ~75° (θ_A/θ_R) are observed (Figure 17). However, as shown in Figure 17, the water contact angles increase and plateau at greater than 0.1 M norbornene concentration. This observation points to surface sensitivity (outermost few angstroms) of the employed contact angle technique.

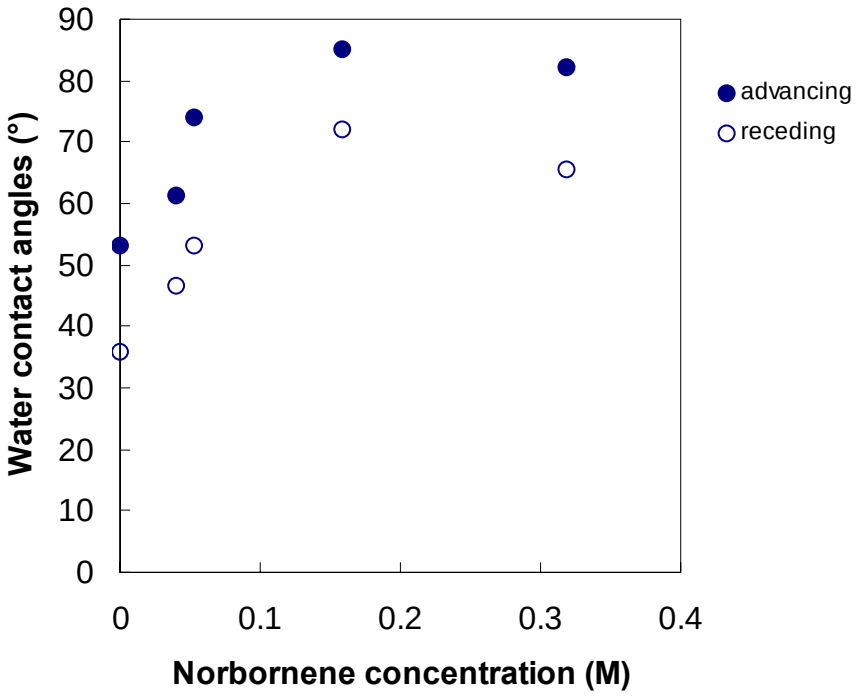

Figure 17. Advancing (●) and receding (○) water contact angles of grafted polynorbornenes prepared using Grubbs catalyst generation II as a function of norbornene concentrations in toluene

Polynorbornenes of up to ~ 70 Å were obtained using Grubbs catalyst generation I and norbornene concentrations of 0.0795 to 0.636 M (Figure 18). As norbornene concentration increases there is a corresponding linear growth of polynorbornenes, which indicates that the Grubbs catalyst generation I initiated polymerization is also living. Even with the highest norbornene concentration of 0.636 M, however, the highest attainable polymer film is only ~ 70 Å thick. This observation lends further insight into the relative reactivities of the Grubbs catalyst generations I and II.

The faster initiation rate of Grubbs generation I gives rise to more reproducible grafted polymer thickness, i.e. individual thicknesses are within ± 15 Å of the reported values and in some cases as low as ± 4 Å. The reproducibility of polymers prepared from generation II pales in comparison: individual values are within as much as ± 270 Å and as low as ± 14 Å of the reported ones. In terms of relative error, the highest relative error for reported values of Grubbs generation II is ± 30% which is greater than the highest relative error of ± 21% for reported values of Grubbs generation I. As mentioned earlier, Grubbs catalyst generation II has a higher propagation rate than generation I that translates to higher molecular weight polymers (Figure 16). These variations in thickness can also be due to differences in grafting density, which will be discussed further.

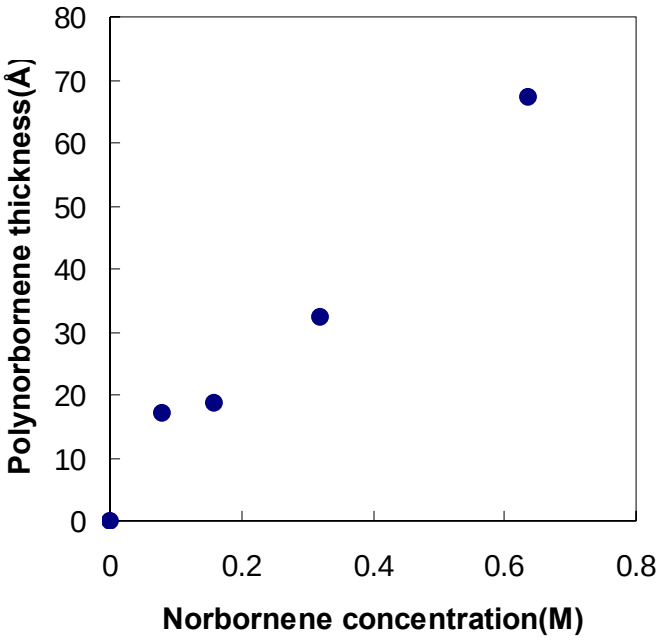

Figure 18. Ellipsometric thickness of polynorbornenes prepared using Grubbs catalyst generation I as a function of norbornene concentrations in toluene

Water contact angles of ~80°/ ~70° (θ_A/θ_R) are obtained for this system (Figure 19). The resulting polymers are not as high in molecular weight (~ 70 Å). That the hysteresis for polymers prepared from generation I is larger than that of generation II indicates relatively inhomogeneous coverage using generation I catalyst. Since contact angle technique detects the outermost few angstroms of the surface, the low contact angle data when the grafted thickness is low, implies that the polymer does not cover the substrate completely and water droplets detect both the grafted polymers and the underlying substrate.

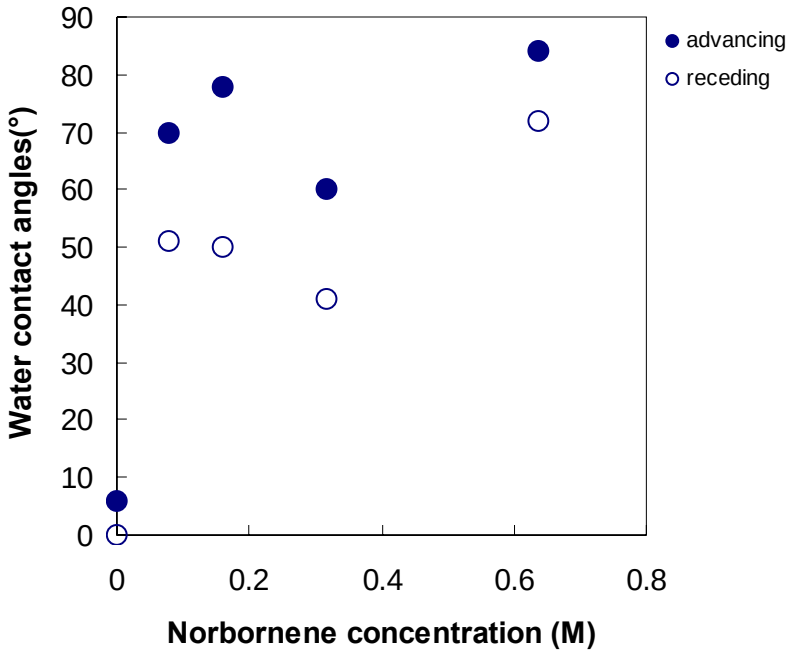

Figure 19. Advancing (●) and receding (○) water contact angles of grafted polynorbornenes prepared using Grubbs catalyst generation I as a function of norbornene concentrations in toluene

Polynorbornenes grafted from both Grubbs catalyst generations I and II containing substrates resulted in living metathesis polymerizations as mentioned earlier (Figure 16 and Figure 18). In a living polymerization, grafted polymer chain length is expected to grow linearly as a function of monomer concentration in the absence of chain transfer and termination reactions. From these concentration dependent studies we see that Grubbs generation II would be the catalyst of choice for the cyclooctadiene system due to higher grafted amounts.

Grafting time also affects the molecular weight of growing polymers. Hence kinetics studies were conducted to ascertain the optimum time for polymerization. High molecular weight polymers up to ~ 600 Å were obtained as grafting time increases when the norbornene concentration was kept at 0.159 M (Figure 20). A plateau region, which corresponds to a thickness of ~ 600 Å is reached after 4 h grafting time. Grafting of norbornene monomer occurred very quickly as ~ 300 Å grafted layer was obtained after 30 min.

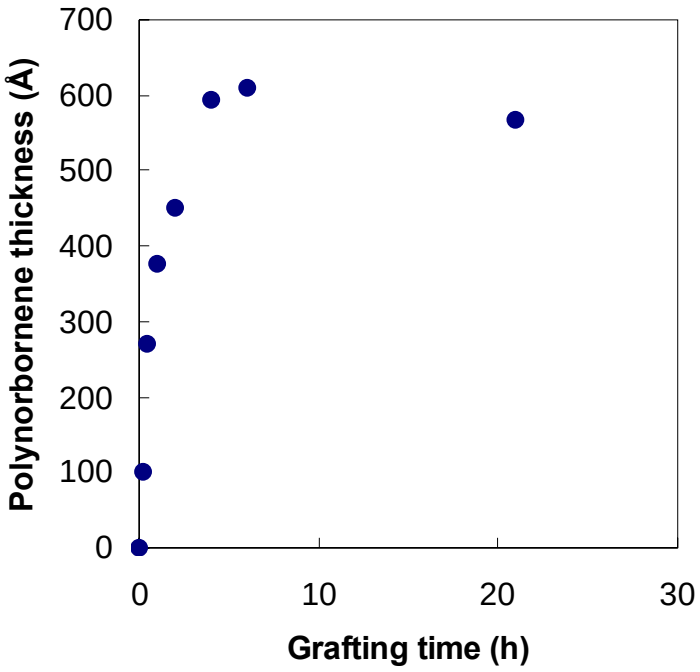

Figure 20. Grafting kinetics study of polynorbornenes grafted from Grubbs catalyst generation II and a 0.159 M norbornene/toluene solution

Water contact angles of these surfaces plateau at ~ 94°/~ 84° (θ_A/θ_R) (Figure 21) once the grafted polymer thickness reaches the sampling depth of

contact angle analysis, which is on the order of a few angstroms. As pointed out in the concentration studies, norbornene being a hydrophobic molecule gives rise to high water contact angles. Contact angles as well as hysteresis vary considerably in Figure 21 and this indicates that there is variation in grafted surfaces.

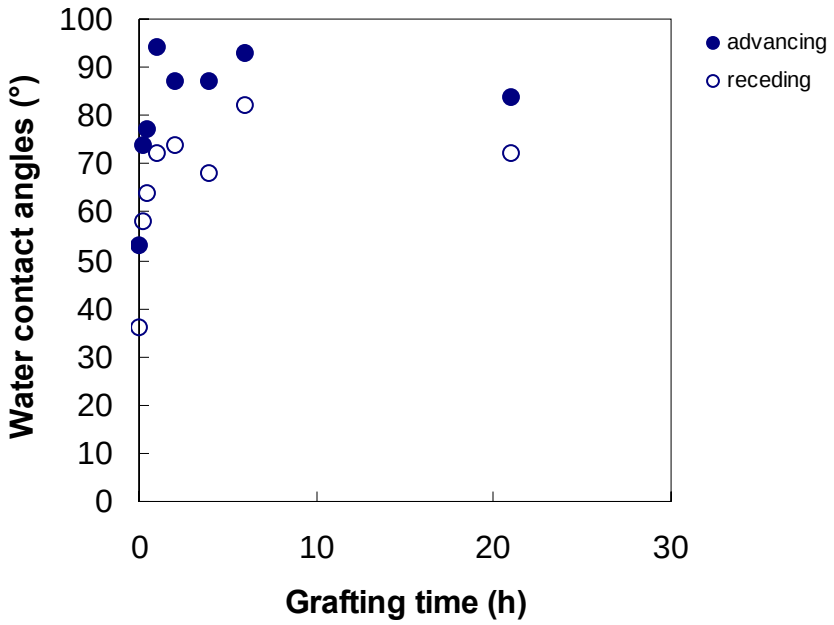

Figure 21. Advancing (●) and receding (○) water contact angles for polynorbornenes prepared using Grubbs catalyst generation II and a 0.159 M norbornene/toluene solution

In contrast, polymers grafted from Grubbs catalyst generation I were up to ~ 70 Å thick at long grafting time (Figure 22). The variations in thickness again point to the differences in reactivities of Grubbs generations I and II. Between grafting times of t = 0 h and t = 8 h polynorbornene thickness increases linearly with increasing grafting time. Grafting of norbornene in

this case occurred slowly in comparison with grafting obtained from generation II (Figure 20). The water contact angles for the Grubbs generation I system increases as grafting time increases and plateaus reproducibly at ~ 82°/ ~ 60° (θ_A/θ_R) (Figure 23).

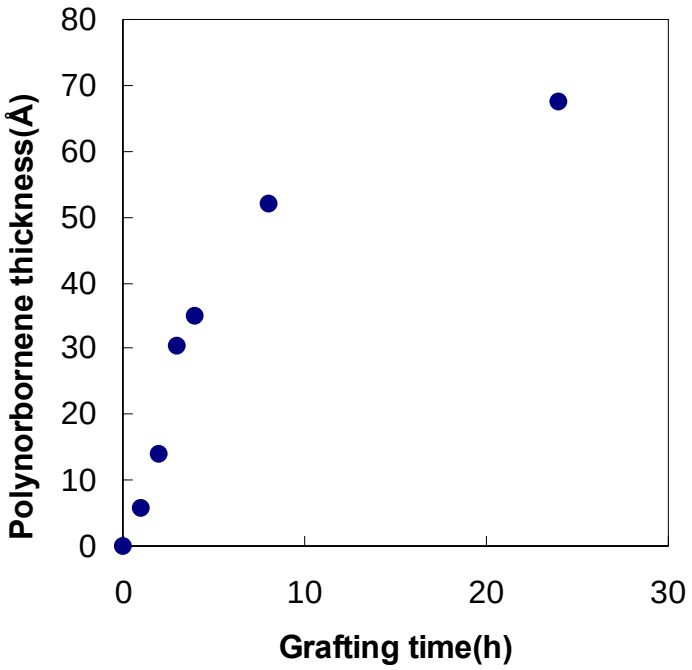

Figure 22. Grafting kinetics study of polynorbornenes grafted from Grubbs catalyst generation I and a 0.636 M norbornene/toluene solution

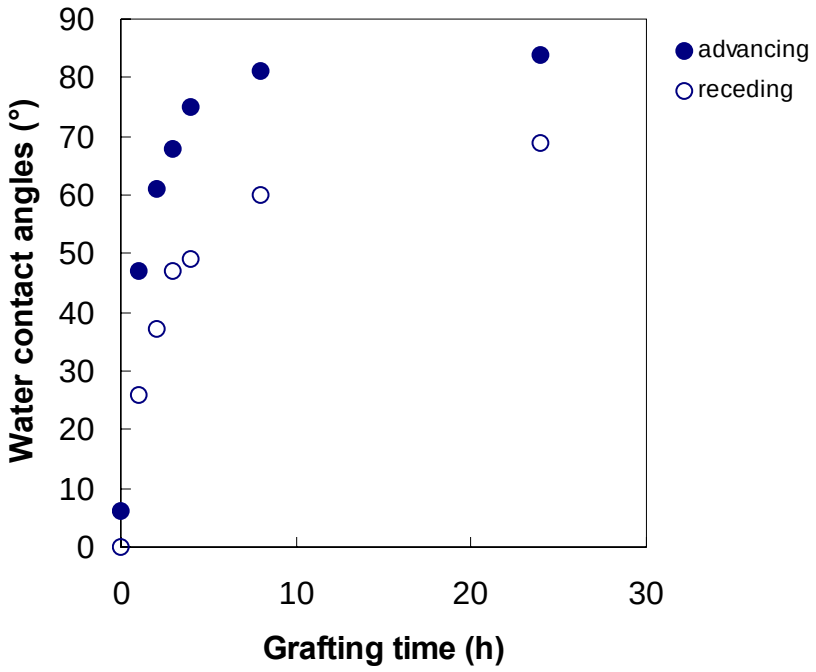

Figure 23. Advancing (●) and receding (○) water contact angles for polynorbornenes grafted from Grubbs catalyst generation I and a 0.636 M norbornene/toluene solution

Grafting density (the density of the surface norbornenyl groups) is controlled by silanization time. Figure 24 shows the grafted polynorbornene thickness as a function of silanization time when the grafting reaction was carried out in 0.159 M norbornene/toluene solution from Grubbs catalyst generation II overnight. Polynorbornene thickness up to ~ 600 Å grafted from a sub- to complete monolayer of norbornenyl groups was obtained. The shape of Figure 24 corresponds well with that of Figure 11. The silane groups deposited to the surface via silanization are initiation sites for polymerization, thus grafting density is controlled by silanization time.

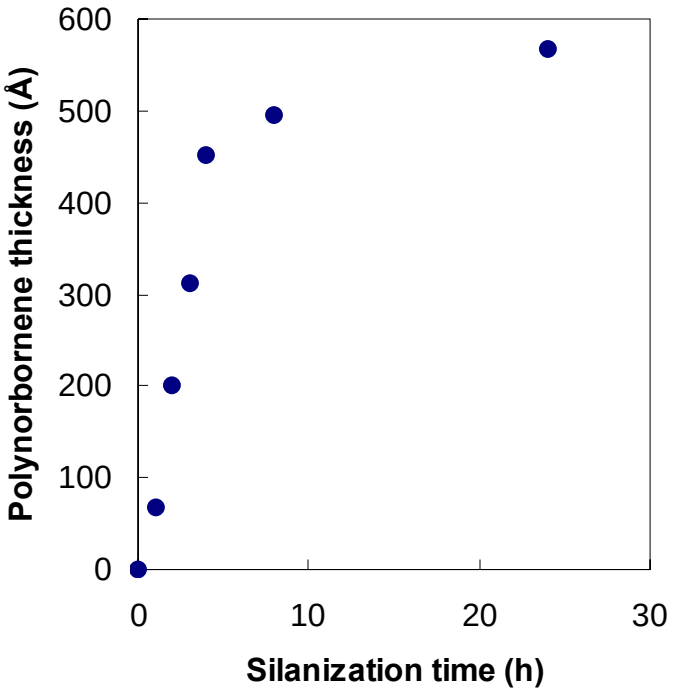

Figure 24. Grafting density of polynorbornenes grafted from Grubbs catalyst generation II and a 0.159 M norbornene/toluene solution

Water contact angle increases as silanization time increases (Figure 25). The low hysteresis exhibited over the entire range of the plot indicates the homogeneity as well as the smoothness of these surfaces. A plateau region of ~ 94°/ ~ 84° (θ_A/ θ_R) is reached after silanization time of 8 h. It is important to note that there is no plateau region in Figure 24 so the plateau region observed in Figure 25 is due to the contact angle technique being insensitive to changes in thicknesses greater than its detection limit.

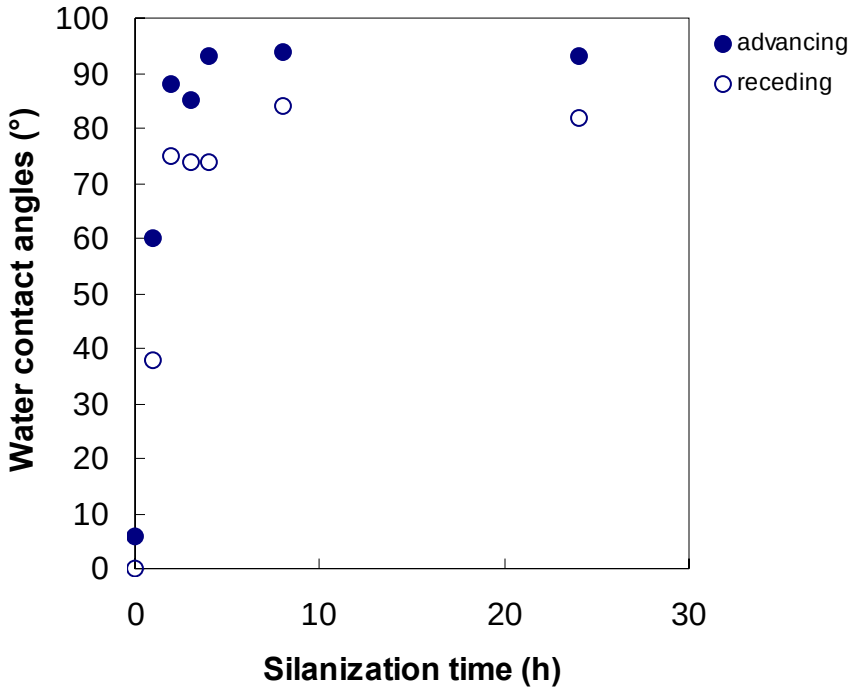

Figure 25. Advancing (●) and receding (○) water contact angles for polynorbornenes grafted from Grubbs catalyst generation II and a 0.159 M norbornene/toluene solution

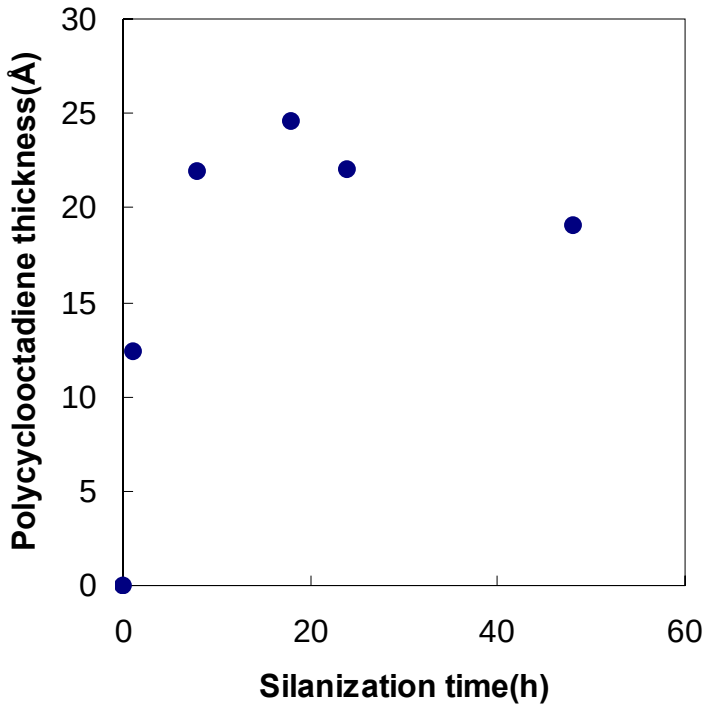

Figure 26. Grafting density of polycyclooctadienes grafted from Grubbs catalyst generation II and neat COD

From preliminary experiments, we found that neat COD afforded the thickest grafted polymer layers due to high monomer concentration. Grubbs catalyst generation II was used because from the norbornene studies it gave higher molecular weight polymers than its generation I counterpart. A grafting density study was conducted to determine the maximum amount of polymer that could be grafted under these conditions. As silanization time increases polycyclooctadiene thickness increases to a maximum of ~ 25 Å, which subsequently decreases to ~20 Å at longer silanization times (Figure 26). Clearly silanization time controls grafted chain density. More explicitly,

if the surface norbornenyl groups are properly spaced they can fulfill their roles as polymerization initiators and result in chain growth. In this case, silanization time of 18 h results in the maximum attainable polycyclooctadiene thickness of ~ 25 Å (Figure 26).

The decrease in polycyclooctadiene thickness at higher grafting density/silanization time is probably due to the polymerization of closer packed surface norbornenyl groups. As a result, fewer norbornenyl groups are available to initiate ROMP of cyclooctadiene. The highest attainable grafting thickness is much less for polycyclooctadiene (~ 25 ± 8 Å) than for polynorbornene (~ 900 ± 270 Å) under the conditions studied. Phosphine dissociation (initiation) is affected by steric and electronic changes[43] and therefore initiation and polymerization of COD does not proceed as fast as those of norbornene due to smaller ring strain of COD.[45]

Cyclooctadiene possessing a low ring strain of 13.28 kcal/mol is often used in assessing the catalytic activity of various catalysts towards ring opening metathesis polymerization (ROMP).[46] In a study conducted by Bielawski et al.[46] they found that ROMP of COD in solution gave rise to polycyclooctadienes with high PDIs (2.1- 2.5) with *trans*-olefin microstructures. The percentage increase of *trans* olefin in the polymer backbone suggests that secondary metathesis isomerization reactions are also taking place.[46] Comparing our results with those obtained by this group lends insight into the mechanism by which ROMP of COD proceeds. The critical

monomer concentration of COD in solution was found to be ~ 0.25 M at 25 ° C.[47,48] In our study, neat COD was employed to minimize chain transfer to solvent and polymer. Backbiting reactions (removal of monomer from the reaction) which take place at longer grafting times can also result in lower molecular weight polymers. Chain transfer and chain termination (backbiting) give rise to short polymer chains. These two processes are much more prominent in polymerization of COD than in that of norbornene.[49]

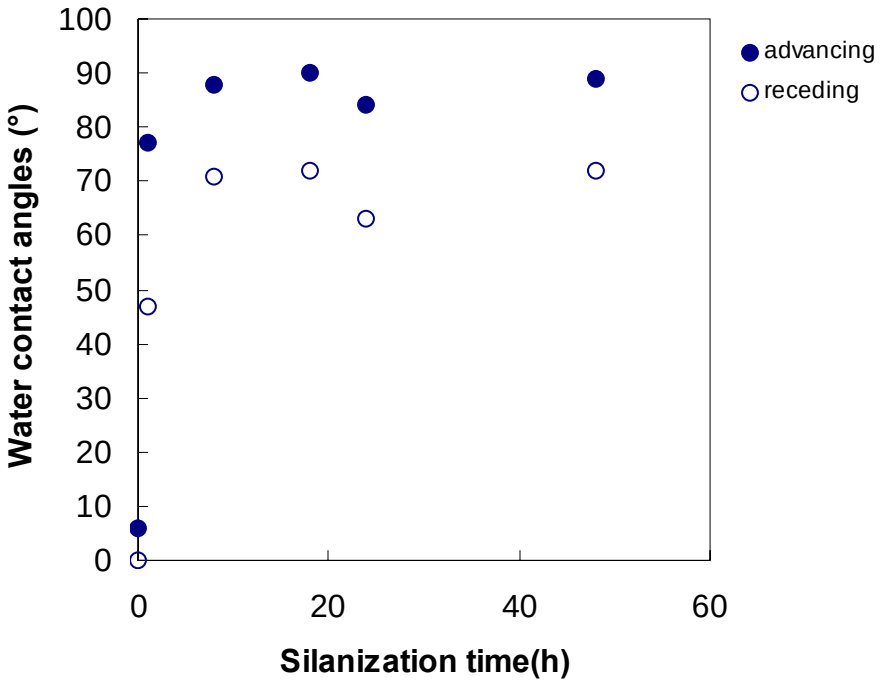

Figure 27. Advancing (●) and receding (○) water contact angles for polycyclooctadienes grafted from Grubbs catalyst generation II and neat COD

Like norbornene, high water contact angles are expected for the polycyclooctadiene layer since the monomer cyclooctadiene is hydrophobic

(Figure 27). High hysteresis indicates that these surfaces are not homogeneously covered.

Polycyclooctadiene surfaces were reacted with an osmium tetroxide containing solution to initiate hydroxylation (Figure 1, Step 4). A kinetics study of hydroxylation was carried out to determine the optimum hydroxylation conditions (Figure 28). Hydroxylation occurs very rapidly; an increase of ~ 8 Å is attained within the first hour of the reaction. A slight decrease in hydroxylated thickness is observed after 6 h. From this graph we deduced that hydroxylation takes place very quickly and that at extended periods of time (≥ 6 h) oxidative chain cleavage more than likely takes place, thereby accounting for the thickness decrease. It should be noted that the reaction mixture was initially (first 30 min) kept at 0 °C to slow down the reaction and thus limit over-oxidation. Therefore, in future experiments, keeping the reaction mixture cooled for longer periods of time could possibly reduce over-oxidation at longer periods of hydroxylation.

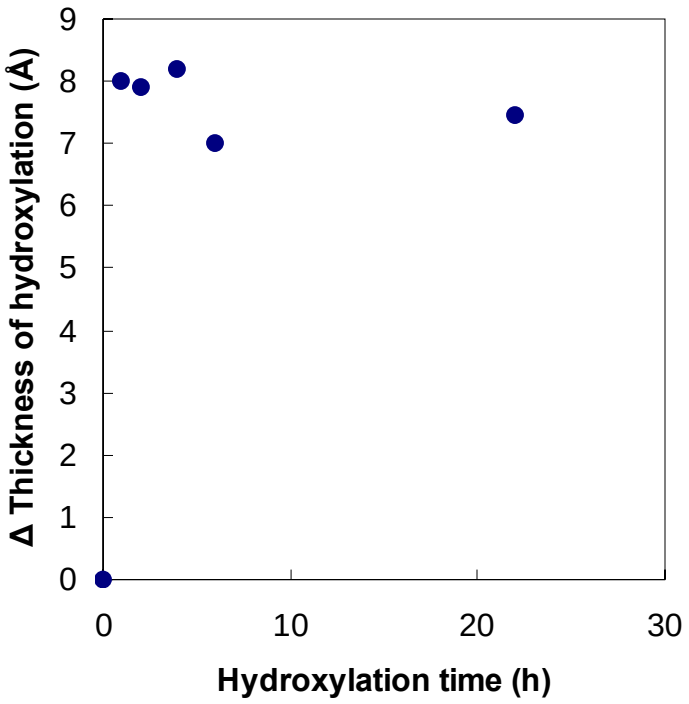

Figure 28. Ellipsometric thickness increase of hydroxylated polycyclooctadiene surfaces prepared from an osmium tetroxide containing solution

Contact angles were expected to be lower since according to our reaction scheme in Figure 1 hydroxylation of polycyclooctadiene gives hh-PVOH, a hydrophilic polymer. However, this was not the case; water contact angles were around ~ 85°/ ~ 55° (θ_A/ θ_R) (Figure 29) slightly more hydrophilic than those of polyCOD (Figure 27) but still fairly hydrophobic. The osmium tetroxide-catalyzed procedure gives rise to *cis* –OH groups and these high contact angles could be due to hydrogen bond formation between the two *cis* –OH groups. As much as a 30° hysteresis is observed for this system which points to the roughness and lack of homogeneity of the prepared surfaces.

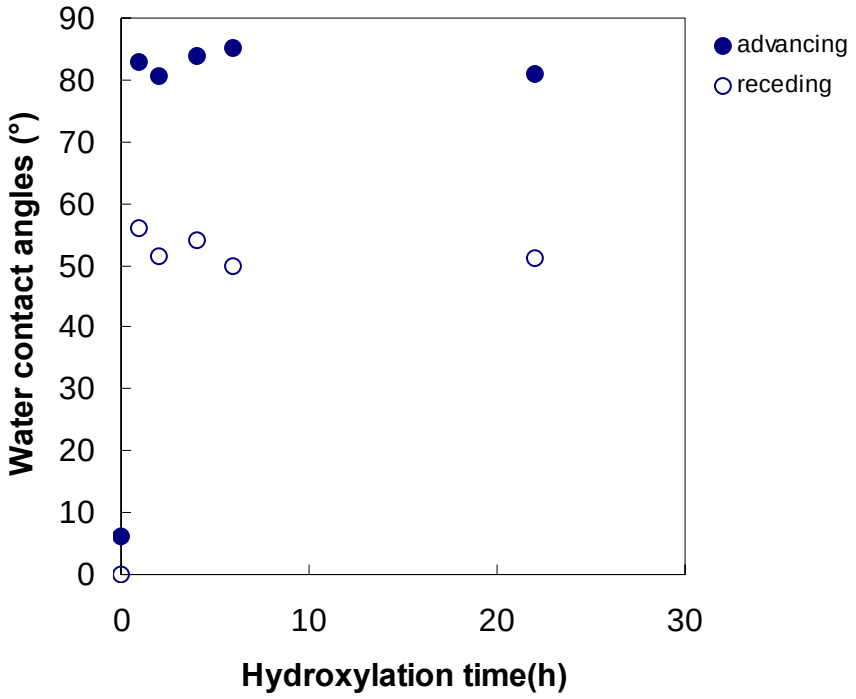

Figure 29. Advancing (●) and receding (○) water contact angles for hydroxylated polycyclooctadiene samples prepared from an osmium tetroxide containing solution

A hydroxylation time of 2 h was chosen for future experiments in accordance with the data presented in Figure 28. Sometimes thickness decrease was observed after hydroxylation, which suggests that a hydroxylation time of 2 h probably also results in over-oxidation of the grafted layer. We decided to quantify the amount of –OH groups formed by labeling the hydroxylated samples with an acid chloride, heptafluorobutyryl chloride (HFBC). If hh-PVOH was indeed prepared, reacting the alcohol groups with HFBC should give rise to fluorinated surfaces as identified by high water contact angles (110°/ 81°) and high ellipsometric thicknesses.[50]

However, the prepared surfaces did not show these high water contact angles. Instead the contact angles obtained were ~ 90°/ ~ 60°. XPS spectra showed low fluorine content (5.6%), which suggested that very little hh-PVOH was prepared (Table 2). Consequently, a different protocol was employed.

In the other approach, polycyclooctadiene surfaces were reacted overnight with *meta*-chloroperoxybenzoic acid (MCPBA) in toluene, which should result in the formation of an epoxide. hh-PVOH was obtained after hydrolysis of the epoxide in aqueous perchloric acid. At each stage the samples were analyzed using ellipsometry, contact angle analysis and XPS (Table 2). Ellipsometric and contact angle analysis for silanized and polymerized samples discussed earlier were also summarized in the table. XPS data for these samples are consistent with results previously presented.

Table 2. Ellipsometric thickness, XPS elemental composition at 45° take-off angle and water contact angles for various substrates of the polycyclooctadiene system

Substrate	Thickness Increase (Å)	C_{1s} (%)	O_{1s} (%)	Si_{2p} (%)	N_{1s} (%)	F_{1s} (%)	θ_A (°)	θ_R (°)
SiO_2	22 ± 2	*	*	*	*	*	6	0
Norbornenyltriethoxysilane	5 ± 1	37.2	36.2	26.6	-	-	53	36
Poly(cyclooctadiene)	25 ±10	30.3	38.8	31.0	-	-	77	43
OsO_4	-18 ± 6	*	*	*	-,*	-,*	94	65
(OsO_4) HFBC	-18 ± 3	33.1	32.3	29.2	-	5.6	90	65
MCPBA	~18	34.1	40	26.0	-	-	57	22
Hydrolysis	30 ± 12	69.7	23.2	7.1	-	-	51	20
(MCPBA-hydrolysis) HFBC	-29 ±10	27.0	34.8	29.8	-	8.6	90	65

Key : - does not contain element, * data was not taken at this take-off angle

The epoxide formed after reaction of poly(COD) with MCPBA is ~ 18 Å thick with water contact angles of 57°/ 22° (θ_A / θ_R). This decrease in water contact angles from 77°/ 43° (θ_A / θ_R) shows that the surfaces are progressively becoming hydrophilic. The increase of the C_{1s} and O_{1s} signals as well as the decrease of the Si_{2p} signal after the reaction indicates the presence of the epoxides. After hydrolysis, a sharp decrease of the Si_{2p} signal is observed; the O_{1s} signal decreases by approximately one-half whereas the C_{1s} signal increases two-fold. The water contact angles are consistent with hh-PVOH hydrophilic surfaces. We also notice the high thickness increase of 30 ± 12 Å for the hydroxylated layer. Intuitively, the oxygen signal should increase as the system becomes more hydrophilic; however, this was not the case. After careful review, we hypothesized that cationic polymerization of the solvent tetrahydrofuran (THF) took place. The high ellipsometric thickness, the significant decrease in the Si_{2p} signal as well as the almost two fold increase of the C_{1s} signal support this hypothesis. Water was chosen as the solvent for cleavage of epoxides to eliminate future cationic polymerization reactions. HFBC was successfully added to the hydroxylated surfaces as indicated by the presence of 8.6% fluorine. The fluorine peak suggests that small amounts of hh-PVOH were actually prepared on the surface. Since hh-PVOH has never been prepared before and thicknesses of poly(COD) are very small in comparison to those obtained from polynorbornene we decided to hydroxylate polynorbornene surfaces for two

reasons. Firstly, the employed hydroxylation protocols have been used in solution and not on surfaces so we wanted to ensure that they worked on surfaces. Secondly, any changes in thicknesses would be more noticeable on these polymerized samples as a result of longer chains/thicker grafted layers.

Hydroxylated polynorbornene surfaces were prepared using osmium tetroxide and epoxidation/hydrolysis protocols (see the Experimental section). These samples were subsequently characterized using ellipsometry, contact angle analysis and XPS. Table 3 shows the comparisons of these methods.

Table 3. Ellipsometric thickness, XPS elemental composition at 45° take-off angle and water contact angles for various substrates of the polynorbornene system

Substrate	Thickness Increase (Å)	C_{1s} (%)	O_{1s} (%)	Si_{2p} (%)	N_{1s} (%)	F_{1s} (%)	θ_A (°)	θ_R (°)
SiO_2	22 ± 2	*	*	*	*	*	6	0
Norbornenyltriethoxysilane	5.0± 0.5	37.2	36.2	26.6	-	-	53	36
Poly(norbornene)	262	92.2	6.7	2.4	-	-	90	80
MCPBA	35	40.3	35.1	24.7	-	-	63	16
Hydrolysis	-30	45.0	32.2	22.9	-	-	72	19
(MCPBA-hydrolysis) HFBC	16	48.3	25.6	12.8	-	13.4	90	28
OsO_4	34	36.4	34.4	29.3	-	-	70	15
(OsO_4) HFBC	19	74.1	12.8	2.4	-	10.6	90	47

Key: - does not contain element, * data was not taken at this take-off angle

After ROMP with norbornene, the intensities of the O_{1s} and Si_{2p} signals decrease whereas the C_{1s} signal increases considerably. The polynorbornene consists of only carbon and no oxygen thus the almost three-fold increase of the C_{1s} signal is expected. As was previously reviewed, high

water contact angles are indicative of a hydrophobic system. The dramatic increase in the O_{1s} signals after reaction with MCPBA is due to the formation of epoxides. The low water contact angles of 63°/ 16° (θ_A/ θ_R) reinforces this point more clearly as the system is becoming more hydrophilic. The increase in the Si_{2p} signal implies polymer chain cleavage due to over-oxidation hence the silicon signal due to the substrate is intensified after epoxidation. The cleavage of the epoxide oxygen bond was accomplished using perchloric acid and water. As was discovered in the cyclooctadiene system, THF undergoes cationic polymerization and therefore water was used as the solvent. The decrease in thickness (-30 Å) observed after hydrolysis confirms the oxidative degradation process. An ellipsometric thickness of 34 Å for *cis*-hydroxylated surfaces prepared using an osmium tetroxide-catalyzed solution was obtained. The carbon signal decreases and oxygen signal increases, both of which correspond well with the hydroxylation process. Again, the increase in the substrate silicon signal is an indication of over-oxidation as was suspected in the reaction with MCPBA. For labeled hydroxylated surfaces, the presence of the F_{1s} signal indicates fluorination. The hydroxylated surfaces prepared from the epoxidation/hydrolysis method had higher fluorine content than those prepared from osmium tetroxide. This higher fluorine content also translates to decreases in O_{1s} and Si_{2p} signals. The low yield of hydroxylated product especially in the osmium tetroxide system could also be due to inertness of the cooxidant, hydrogen peroxide, toward hindered olefins.[51]

The less successful hydroxylation of polycyclooctadienes using either osmium tetroxide or MCPBA/hydrolysis is probably due to the oxidative degradation under the conditions used, as shown in the reactions with polynorbornenes. The thickness of grafted polycyclooctadiene (< 25 Å) is too thin to "tolerate" such degradative processes. The two methods described to prepare *cis* –OH groups and *trans* –OH groups have been shown above to yield surface –OH groups in the polynorbornene system. Optimization of reaction conditions is underway to maximize hydroxylation and minimize degradation in the polycyclooctadiene system.

CONCLUSION

Norbornene has been grafted to surfaces via ROMP using both Grubbs catalyst generations I and II in a living fashion. The Generation II catalyst is more reactive and up to ~ 900 Å thick polymer films were obtained. However, more uniform polymer chain lengths are obtainable using generation I catalyst. Grafting density was controlled by silanization time; molecular weight/polymer chain length was controlled by monomer concentration and grafting kinetics. Grafting of cyclooctadiene was much more challenging. Even when neat cyclooctadiene and more reactive generation II catalyst were used, only up to ~ 25 Å thick films were grafted via ROMP probably as a result of extensive chain transfer and termination. Intermediate to high grafting density promotes grafting for cyclooctadiene.

Hydroxylation studies using both osmium tetroxide and MCPBA/hydrolysis methods are in progress so that hydroxylation is maximized and degradation is kept at a minimum.

REFERENCES

1. Rouhi A. M. *Chemical Engineering News* **2000**, 33.
2. Brash, J. L. *Journal of Biomaterials Science Polymer Edition* **2000**, *11*, 1135.
3. Castner, D. G.; and Ratner, B. D. *Surface Science* **2002**, *500*, 28.
4. Ishihara, Y.; Ishihara, K.; Nakabayahsi, N. *Recent Res. Devel. In Polym. Sci.* **1997**, *1*, 37.
5. Ishihara, K.; Ueda, T.; Nakabayashi, N. *Poly. J.* **1990**, *22*, 355.
6. Harris, J. M. *Poly(Ethylene Glycol) Chemistry: Biotechnical and Biomedical Applications*, Plenum Press, New York, **1992**.
7. Sofia, S. J.; and Merrill E. W. In Poly(Ethylene Glycol) Chemisty: Biotechnical and Biomedical Applications; Harris, J. M., Ed.; American Chem. Society: Washington DC, 1997; p. 342.
8. Ishihara, K.; Nomura, H.; Mihara, T.; Kurita, K.; Iwaski, Y.; Nakabayashi, N. *J. Biomat. Mater. Res.* **1998**, *39*, 323.
9. Iwasaki, Y.; Sawada, S.; Nakabayashi, N.; Khang, G.; Lee, H. B.; Ishihara, K. *Biomaterials* **1999**, *20*, 2185.
10. Hasegawa, T.; Iwasaki, Y.; Ishihara, K. *Biomaterials* **2001**, *22*, 243.
11. Morra, M. *J. Biomater. Sci. Polymer Edn.* **2000**, *11*, 547.
12. S. Alexander, *J. Phys.* **1997**, *38*, 977.

13. De Gennes, P.G, *Scaling Concepts in Polymer Physics*, Cornell University Press, Ithaca, NY, **1979**.

14. De Gennes, P.G. *Ann. Chim*. 1987, *77*, 389.

15. Jeon, S. I.; Lee, J. H.; Andrade, J.D.; De Gennes, P.G. *J. Coll. Inter. Sci* **1991**, *142*, 149.

16. Jeon, S.I.; Andrade, J.D. *J. Coll. Inter. Sci.* **1991**, *142*, 159.

17. Szleifer,I. *Curr. Opin. Coll. Interf. Sci.* **1996**, *1*, 416.

18. Szleifer,I. *Biophys. J.* **1997**, *72*, 595.

19. Szleifer,I. *Physica A.* **1997**, *244*, 370.

20. Szleifer,I. *Curr.Opin. Solid State Mater. Sci*. **1997**, *2*, 337.

21. Prime, K. L., and Whitesides, G. M. *J. Am.Chem. Soc*. **1993**, *23*, 10714.

22. Besseling, N.A.M., and Scheutens, J. M. H. M., *J. Phys. Chem*. **1994**, 98, 11597.

23. Besseling, N.A.M. *J. Phys. Chem*., **1994**, *98*, 11610.

24. Besseling N.A.M. and Lyklema, J. *J. Pure Appl. Chem*. **1995**, *67*,881.

25. Besseling, N.A.M., *Langmuir* **1997**, *13*, 2109.

26. Special Issue, *J. Biomater. Sci. Polym. Edn.* **1999**, *10*, 1011.

27. McCarthy, T. J. and Fadeev, A. Y. *Langmuir* **1999**, *15*, 7238.

28. McCarthy, T. J.; Russell, T. P.; Fadeev, A. Y.; Stafford, C. M.; *Langmuir* **2001**, *17*, 6547.

29. McCarthy, T. J.; Fadeev, A. Y. *Langmuir* **2000**, *16*, 7268.

30. Ilker, M. F.; Coughlin, B. E. *Macromolecules* **2002**, *35*, 54.

31. Verpoort, F.; Couchez, K.; Opstal, T. *Adv. Synth. Catal.* **2003**, *345,* 393.

32. Stevens, M. P. *Polymer Chemistry: An Introduction*, Oxford University Press, Oxford, **1999**.

33. Scherman, O. A.; Grubbs, R. H. *Synthetic Metals* **2001**, 431.

34. Rutenburg, I. M.; Scherman, O. A.; Grubbs, R. H.; Jiang, W.; Grafunkel, E.; Bao, Z. *J. Am. Chem. Soc.* **2004**, *126*, 4062.

35. Tompkins, H. G. *A User's Guide to Ellipsometry*, Academic Press, San Diego, **1993**.

36. Andrade, J. D. *Surface and Interfacial Aspects of Biomedical Polymers, Surface Chemistry and Physics*, Plenum Press, New York, **1985**.

37. Johnson, R. E. Jr.; Dettre, R. H. *Surface Colloid Science* **1969**, *2*, 85.

38. Sheardown, H. *J. Biomater. Sci. Polymer Edn.* **2002**, *13*, 593.

39. Weck, M.; Jackiw, J. J.; Rossi, R. R.; Weiss, P. S.; Grubbs R .H. *J. Am. Chem. Soc.* **1999**, *121*, 4088.

40. Ivin, K. J.; Mol, J. C. *Olefin Metathesis and Metathesis Polymerization*, Academic Press, London, **1996**.

41. Kim, N. Y.; Jeon, N. L.; Choi, I. S.; Takami, S.; Harada, Y.; Finnie, K. R.; Girolami, G. S.; Nuzzo, R. G.; Whitesides, G. M.; Laibinis, P. E. *Macromolecules* **2000**, *33*, 2793.

42. Leyden, D, E.; Ed. *Silanes, Surfaces and Interfaces*; Gordon and Breach: New York, 1986.

43. Love, J. A.; Sanford, M. S.; Day, M. W.; Grubbs, R. H. *J. Am. Chem. Soc.* **2003**, *125*, 10103.

44. Choi, T.; Grubbs, R. H. *Angew. Chem. Int. Ed.* **2003**, *42*, 1743.

45. Breitenkamp, K.; Simeone, J.; Jin, E.; Emrick, T. *Macromolecules* **2002**, *35*, 9249.

46. Bielawski, C. W.; Grubbs, R. H. *Angew. Chem. Int. Ed.* **2000**, *39*, 2903.

47. Suter, U.W.; Höcker, H. *Makromol. Chem.* **1988**, *189*, 1603.

48. Höcker, H.; Reimann, W.; Reif, L.; Ribel, K. *J. Mol. Catal.* **1980**, *8*, 191.

49. Bielawski, C. W.; Benitez, D.; Grubbs, R. H. *J. Am. Chem. Soc.* **2003**, *125*, 8424.

50. Ndong, R. S. Personal communication.

51. Minato, M.; Yamamoto, K.; Tsuji, J. *J. Org. Chem.* **1990**, *55*, 766.